

Case study: Performance analysis and development of robotized screwing application with integrated vision sensing system for automotive industry

*International Journal of Advanced
Robotic Systems*

May-June 2020: 1–23

© The Author(s) 2020

Article reuse guidelines:

sagepub.com/journals-permissions

DOI: 10.1177/1729881420923997

journals.sagepub.com/home/arx

Milan Sága¹, Vladimír Bulej² , Nadežda Čuboňová², Ivan Kuric²,
Ivan Virgala³  and Manfred Eberth²

Abstract

Industrial cameras starting to play a significant role in current industrial environment and they represent a strong tool for robotics mainly in cases when they are combined with high-speed robots. However, there are still some difficulties in vision system integration. The capability of such system (e.g. assembly or technological system) depends on several factors, for instance, the camera position, lightning conditions, pattern recognition algorithms, precise setup, as well as well-trained programmer and engineer. The skills of the engineering staff and the precise analysis of conditions and process requirements seem to be crucial for successful solution, what was proved also in our experimental test. The main aim of the article is development and complex performance analysis of robotized screwing application with integrated vision system, concretely the case study of automated assembly system in automotive industry—bolting tightening robotized station as a part of car seat assembly process. The main key elements of the designed workplace are industrial robot FANUC M-20iA/20M with integrated iRVision system containing the industrial camera Sony XC-56. The real influence of inaccuracies during the design process, gradual “step-by-step” refinement, and final influence of all changings on the final quality and efficiency of designed system was demonstrated. At the end, we reached the point where the total number of screwing operations with NOK results (not OK / negative results) is about six single negative results per day, which represents less than 0.1% of all recognitions (overall reliability is higher than 99.9%).

Keywords

Robot vision, camera sensing system, robotized screwing application, case study, performance evaluation of vision systems, object recognition, automotive industry, FANUC iRVision 2D, Desoutter CVI3 assembly system, camera Sony XC-56

Date received: 16 December 2019; accepted: 26 March 2020

Topic: Vision Systems

Topic Editor: Antonio Fernandez-Caballero

Associate Editor: Martin Grossman

Introduction

Several authors (for instance, Küpper and Kuhlmann¹) mentioned that advanced digital technology is already used in industry; however, with Industry 4.0, it will transform the production to smarter automation in various ways via installing of smart robots, sensors, using of collaborative robots, applying production simulations, and so on.

¹ Department of Applied Mechanics, Faculty of Mechanical Engineering, University of Žilina, Žilina, Slovakia

² Department of Automation and Production Systems, Faculty of Mechanical Engineering, University of Žilina, Žilina, Slovakia

³ Department of Mechatronics, Faculty of Mechanical Engineering, Technical University of Kosice, Kosice, Slovakia

Corresponding author:

Vladimír Bulej, Department of Automation and Production Systems, Faculty of Mechanical Engineering, University of Zilina, Univerzitna 1, SK-010 26, Zilina, Slovakia.

Email: vladimir.bulej@fstroj.uniza.sk



Creative Commons CC BY: This article is distributed under the terms of the Creative Commons Attribution 4.0 License (<https://creativecommons.org/licenses/by/4.0/>) which permits any use, reproduction and distribution of the work without

further permission provided the original work is attributed as specified on the SAGE and Open Access pages (<https://us.sagepub.com/en-us/nam/open-access-at-sage>).

Nowadays, there are constantly appearing new applications in robotics and its specific branch, namely vision guided robot systems (VGR systems) where the so-called machine vision (MV) systems have found their strong usage. General VGR system is basically any robot system where the feedback for precise robot navigation to a variable target position is provided via at least one industrial camera.^{2,3} As a result, their application can reduce total costs and make it possible to solve tasks that would not be possible without the usage of such cognitive sensors. The main motivation for VGR systems usage in robotics is to replace human cognitive capabilities (visual sense and decision-making) to perform wide variety of tasks where the ability to adapt to variable conditions is strongly required or mandatory. Their main purpose is obtaining information and on this basis controlling processes or machines via proper interpretation of scene's image achieved through the optical contactless sensing system.

Modern advanced sensing systems based on "smart camera sensors" have been quickly spread into many fields of industry, such as general process control,⁴ general object identification and recognition,⁵ quality check (Stejskal, Bayraktar, Alghamdi),⁵⁻⁷ reading texts and codes (e.g. car identification plate),^{8,9} face recognition (Park),¹⁰ robot control via gestures¹⁰ and general pose control of robots using visual servoing,³ visual navigation of single/multiple mobile robot/s (Kim, Ostertag, Mikulova, Roberti),¹¹⁻¹⁴ collision detection and perception (Lehnhardt),¹⁵ many applications in food industry, and online process control and monitoring (Kosinar)¹⁶ using component recognition (Stipancic, Scholz-Reiter).^{17,18} Smart sensors are key elements for visual inspection of parts or visual navigation of robots for assembly tasks that has been manually done by human operators before.

Inclusion of large data sets is often necessary by the nature of cognitive sensory systems. Proper simulation can be utilized with both real pictures and synthetic images to minimize any negative effects of processing such extensive data sets.¹⁹ Bayraktar and his colleagues⁶ proposed method for efficient processing of hybrid image data sets. Due to the nature of the processed data, VGRs must be able to learn and to "understand" the scene in real world, so they are often closely related to different approaches of artificial intelligence. Since they show better results for some specific tasks, many studies are being conducted on neural networks application (Park)¹⁰ or combination of machine learning algorithms.^{2,8,10,20}

While the MV market offers various types of vision systems, such as *PC-based systems*, *Smart Camera vision system*, and *hybrid Smart Camera vision system*,³ for most tasks, VGR systems are sufficient to apply two-dimensional (2D) MV systems based on data collection from single camera.^{15,20} On the other hand, for more advanced tasks (like, e.g. the so-called bin-picking), it preferred the three-dimensional (3D)—stereo camera system.^{21,22} Although the sensor Kinect has gained notoriety for 3D

scanning of industrial robot environment (for instance, Bobovsky, Ghani),^{23,24} it is not entirely appropriate for such robot navigation where the high positioning accuracy is required. In general, this type of sensor uses an indirect method of sensing the world based on the 3D space transformation into 2D image information, whether perpendicular or perspective projection is defined. Mario Claer²⁵ pointed out that it is becoming increasingly important for the robotic system to be able to perceive its surroundings in 3D in specific areas. Scanner based on light detection and ranging method for measuring distance of obstacles (LiDARs) and other kind of 3D scanners are therefore often used for similar tasks, even though their field of vision is smaller. This disadvantage can be eliminated in several ways, mostly by mounting on different types of rotary platforms.

Among the advanced camera systems, we can classify above all visual navigation of mobile robots and self-driving cars, human body gesture or face keypoints recognition, and so on. The application of MV system in autonomous navigation of mobile robots and self-driving cars is mentioned in authors such as Kim,¹¹ Claer,²⁵ and others. Jeong-Hyun Kim¹¹ proposed the so-called Self-Organizing Map algorithm to obtain suitable data about the position of objects in space based on depth data from a stereo camera. This system is used to analyze the front part area of a vehicle in forms of several candidate planes. Kocic et al.,²⁶ in their study, presented a short overview of available sensors and basic rules for sensor fusion in area of autonomous vehicles navigation as well. Park⁴ and many others focused their research on MV for human body gesture or face keypoints recognition. Research in this area becomes popular in the last 10 years mainly for robot control. Other interesting application of MV is presented in article written by Christie et al.,²⁷ where a vision alarm system for rock crusher is presented. Bozek²⁸ and his colleagues proposed a new method for analytic solution of trajectory calculation for precise robot control along the advanced trajectories. Bako et al.²⁹ and Dizo³⁰ are dealing with increasing the efficiency of robotized production lines including grasping of object via simulation tools, which can significantly reduce the bottleneck occurrences and handling accidents. Labudzki³¹ created the review article about capabilities and applications of MV systems, while Kim⁹ focused on neural network usage for MV.

This article describes a case study about performance analysis and development of robotized screwing application with integrated vision sensing system for automotive industry. Imaging analysis with *iRVision* systems is applied to finding the real position of screws in the target region. In this article, we have designed and tested the *Recliner bolting station* for the task of autonomous screwing operation of four bolts connecting the back frame with the seat frame of the car seat. The key element of assembly process is application of vision guided robotic system for screwheads recognition and obtaining their precise current position within defined range. The functionality of all key

Table 1. Basic requirements defined by the customer.^a

Basic requirements defined by the customer	
Parameter	Value
Initial position setting of the seat in axis X	0 mm (seat is at the end of guidance, in rear position)
Maximum range in axis X (horizontal setting)	cca + 20 mm (forward)
Initial position setting of the seat in axis Y	0 mm (seat is at lowest possible position)
Maximum range in axis Y (vertical setting)	Screw 4: approximately Y = 288 mm from pallet top surface
Maximum total cycle time (time “1st seat enter assembly position – 2nd seat enter assembly position”)	cca + 20 mm (upward)
Maximum working cycle time (time “robot START – robot STOP”)	Approximately 45 s
Type of seat	Approximately 35 s (later under 25 s)
Maximum number of NOK results (due to any reason)	All seats in production portfolio of the customer (manual/power seat, different material equipment, etc.)
Required torque range at all screws	Up to 10 screws per day (possible reasons: wrong detection, obstacle between screwdriver and screwhead, light conditions, etc.)
	4.5–5.5 kgfm/44.1–53.9 Nm

^a“Car set” contains a couple – one left and one right seat.



Figure 1. The Bolting station definition—basic structure of the workcell (left), detail of scanned area for finding of screws (right down), screwing order definition (right up), and detail on prescrewed bolt in position how is entering the station (middle).

features—station design, chosen equipment, designed recognition procedure, proposed methods, and the designed program—was proved via experimental verification and for more than 2 years run as a part of whole production line.

Task formulation and basic workplace configuration

The task is to design and implement the VGR system for bolting operation—tightening of four screws (bolts) connecting the back frame and bottom frame of the seat. Final cell will replace the human operator from economic, as

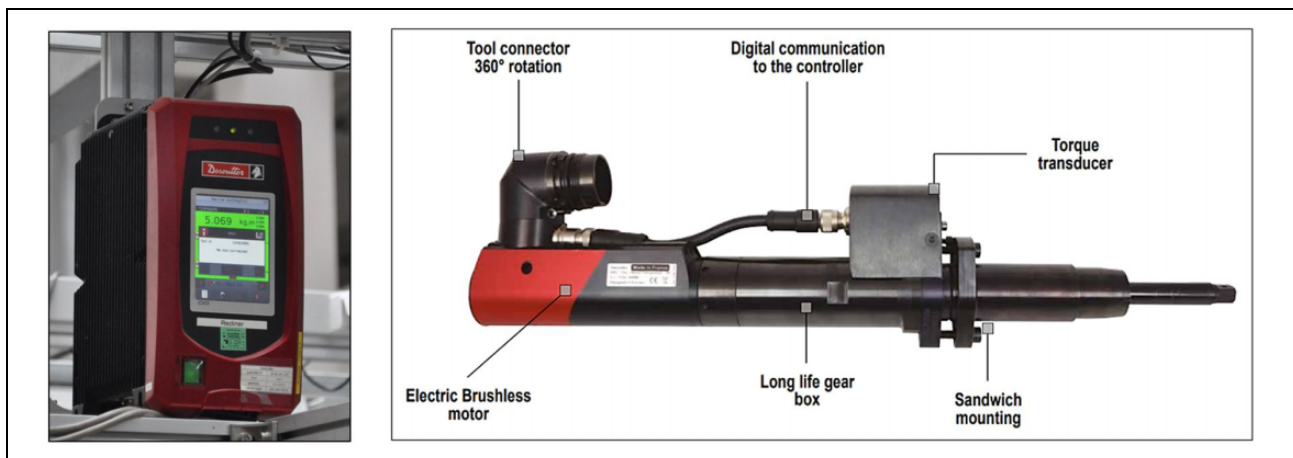
well as ergonomic reasons. Whole system must be designed as an integral part of existing assembly line for passenger car seats produced by an external customer. Total average production capacity of the production line is defined as 1000 “car sets” (pair of front seats – one left (LH) and one right (RH)) per day. The real production capacity can vary with respect to the customer requirements. It means that average number of “screwing cycles” is about 8000 per day (1000 LH + 1000 RH and for each of them four screws).

The basic requirements are summarized in Table 1. The workcell and the assembly components are shown in Figure 1.

Table 2. Basic technical specification of robot FANUC M-20iA/20M.³³

FANUC M-20iA/20M (high inertia version)

Parameter	Unit	Value	Parameter	Unit	Value
Maximum load capacity at wrist	kg	20	Mounting position	—	Floor
Maximum reach	mm	1813			Upside down
Controlled axes	—	6			Angle
Repeatability	mm	±0.03 ^a	Protection—body	—	IP54
Mechanical weight	kg	250	Wrist and J3	—	IP67
J6 moment/inertia	Nm/kgm ²	30.0/1.01	Voltage 50/60 Hz 3P	—	380–575
Robot footprint	mm	343 × 343	Controller	—	R30iB

^aBased on ISO9283.**Figure 2.** Tool for screws tightening—electric spindle Desoutter EFDE³⁴ (right) and its control unit CVI3 (left).

Workplace structure and equipment

The first goal is to design the robotized bolting workcell, concretely to select suitable equipment and to design all systems to work as one fully integrated automated robotized assembly system according to the requirements (Table 1). So it will be necessary to combine utilizing a six-axis FANUC robot, 2D vision system, and a conveyor system of the production line. The station is under the supervising of higher level control system for whole production line—so it has to be synchronized with all other processes by manufacturing execution system (MES) system. The main reason why VGR system was required is that the seat setting can vary regarding the previous operations—they can enter the bolting station with different setup in both directions—position of height adjustment lever as well as in horizontal direction.

Robot FANUC M-20iA/20M

The company FANUC Robotics provide a variety of robots for different purposes.³² We decided to apply the robot FANUC M-20iA/20M³³ with R-30iB controller series in this project. Chosen version of the robot is capable to do degrees of freedom (6-DOF) motion of end effector within

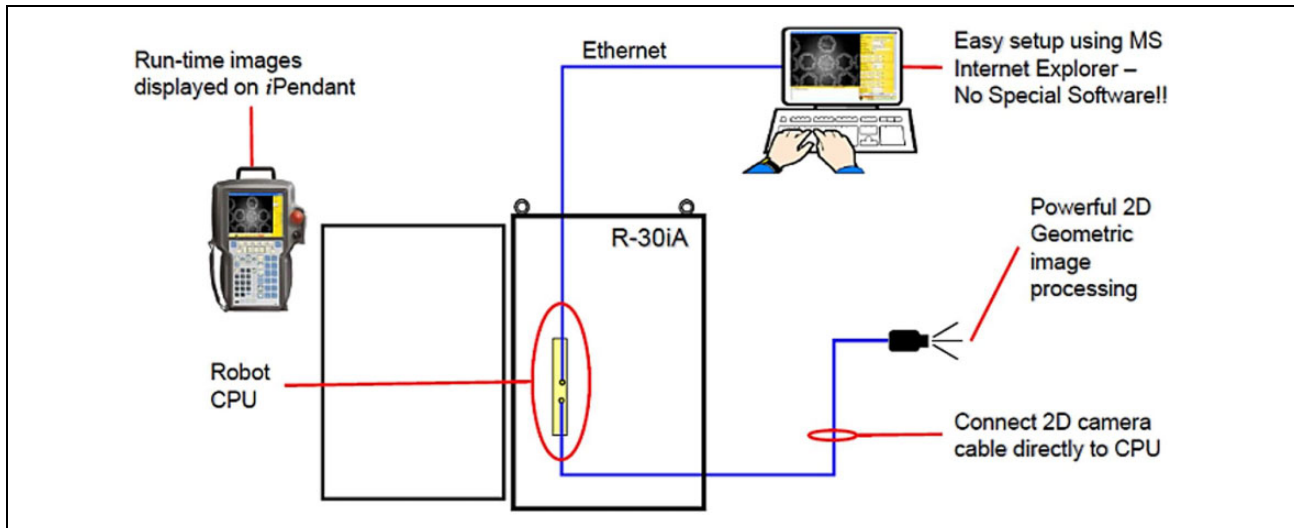
the spherical workspace with maximum diameter 1860 mm, while maximum payload is limited to 20 kg included the end effector (see Table 2). The main advantage lies in the effective combination of stiffness, payload, reach, and axis speed. FANUC R-30iB robot controller is compact and easy to integrate into single robot production cells and it is ready for intelligent functions such as vision, force, and interference check as standard. We chose the version with “Mate Cabinet,” which is powerful and self-contained and has been designed specifically for M series and LR-Mate robots. For robot control, setting and programming were applied the teach pendant with touch screen.

Screwdriver—spindle Desoutter EFDE

The inline fixtured spindle Desoutter EFDE 51-70 (Figure 2; Table 3) as the main tool was used—part of Desoutter CVI3 assembly system developed especially for automotive industry. Dedicated to meet the demanding requirements of this industry segment, the CVI3 platform assures the robust screwdriver design based on brushless motor combined with the torque transducer and traceability of all the safety critical application process. The integration of error proofing modules is easy to adapt to each application.

Table 3. Basic technical specification of electric spindle Desoutter EFDE 51-70.³⁴

Desoutter EFDE 51-70 (CVI-3 electric assembly systems)					
Parameter	Unit	Value	Parameter	Unit	Value
Part number	—	6151658680	Net weight	kg	5.35
Model	—	EFDE 51-70	Length	mm	540
Output drive	“	1/2	Side to center	mm	51
Free speed	rpm	816	Telescopic	mm	50
Torque range	Nm	20–80	Range of electric assembly system		CVI3

**Figure 3.** General schema of FANUC *iRVision* system and connection of peripheral devices.³³

Vision system—basic structure

The main aim of vision system is to provide the necessary data about shape and position of parts beneath the camera's view range to the robot controller. FANUC robots are teaching-playback robots.³⁵ In a teaching-playback system, specific tasks are taught to robots in advance, which then in turn work exactly as they are taught according to the robot program.^{36,37} This means that, if you want the robot to do any operation with specific component in the same way, you need to place every component at exactly the same position. As a result, the production flexibility increases due to the eliminated need for expensive positioning fixtures. Unfortunately, this is not true in our case due to some different setting of every seat in production line.

The FANUC *iRVision* system is a fully robot integrated visual sensor system designed to eliminate such restrictions.^{38,39} *iRVision* system uses one or more cameras to find the precise position and orientation (or other desired parameter, e.g. color, different size/scale factor) of each object within the scene and modifies preprogrammed robot trajectory. So that the robot can do the same operation even if the position (orientation, etc.) of the objects is different from their position set when the robot program was taught.³⁸ The *iRVision* application solution can be implemented on any FANUC industrial robot equipped with

suitable hardware card for its connection and can be customized (different capability 2D, 2½D or 3D vision, different tasks, etc.). The main advantages and reasons for application of integrated *iRVision* system are reduced capital and operating costs, reduced complexity of whole system, stable running due to the elimination of third-party hardware and software features, and high speed of vision communication and processing through robot backplane.

The 2D *iRVision* system is sufficient for the conditions of our application where it finds parts and their precise position and orientation (X, Y, Z, and R). Our *iRVision* system (schema in Figure 3) composed from camera Sony XC-56, the lens, proper light source, Ethernet cable/JRL6A port, and software platform *Web server* was installed on the FANUC M-20iA/20M robot to serve the robot guidance and to find position of screwheads.

Camera. Here we applied the single camera *Sony XC-56* (see Figure 4; Table 4) with lens fixed focus length, F1.8-1.4. It was not necessary to choose zoom lens type due to robot-mounted camera, so the proper focal distance can be reached by the position of the robot arm itself. Camera is mounted on the robot arm end effector—it is carried on common holder with the screwdriver (see Figure 4, right). This holder is connected with the flange of robot axis J6.



Figure 4. Camera Sony XC-56—rear and front view (left/middle) and its mounting on common holder with the screwdriver (right).

Table 4. Basic technical specification of camera Sony XC-56.⁴⁰

B/W progressive scan camera Sony XC-56

Parameter	Unit	Value	Parameter	Unit	Value
Body dimensions	mm	29 × 29 × 30 (W × H × D)	Weight	g	50
Sensor type	—	1/3 type progressive scan CCD with square pixels	CCD vertical drive frequency	kHz	15.734 ± 1%
Speed of image capturing	Frames/s	30	Electronic shutter	s	1/100 to 1/15,000
Image size	—	VGA resolution (659 × 494 pixels)	Ext. trigger shutter speed	s	1/4 to 1/100,000
High S/N ratio:	dB	58	Minimum illumination:	lux	0.5 (at F1.4)
Lens mount	—	C-Mount	Power	W	1.5
Voltage	V (DC)	12 (+10.5 to 15)	Op. temperature	°C	−5 to 40

W: width; H: height; D: depth; CCD: charge-coupled device; VGA: video graphics array; Ext.: external; DC: direct current; Op.: operating.

The optical axis of both camera and screwdriver is parallel and offset 90 mm each other. The *Sony XC-56* is a monochrome camera module that incorporates a 1/3 type progressive scan CCD. It has VGA resolution (647 × 493 pixels) output at 30 fps or optionally 60 fps. Various settings are available on the rear panel.

Lightning and filtering. The main objective of lighting for MV systems is to create the most favorable conditions for quality detection of required objects, in particular maximize the contrast between objects of interest and their background. In general, these conditions can be achieved by choosing suitable illumination source or combination of sources,⁴¹ its or their position, light intensity, diffusion parameter, color, and so on.^{3,8} Due to the difficult light condition around the production line, it was necessary to use individual light source. We were thinking about several alternatives:

- One light source carried at the robot end effector (moving with the camera).
- One light source carried at the robot end effector and one static diffuse bar light from above.
- Combination of one light source carried at the robot end effector, one static diffuse bar light from the ceiling, and one light source focused on each side of the seat mounted on the protection cage.

We have decided for second alternative with respect to ensure reducing costs, as well as to avoid possible collision of two side light sources with other objects within the protection cage or collision with conveyor itself. The standard light source commonly used in a given production line was chosen as the upper diffuse light source.

In our case, it is not possible to apply other lightning methods, such as backlight, side light, and so on. It is also not possible to change the properties and structure of top surface of the frame parts, which creates the background of the screws. So, the proposed vision system must therefore be robust enough to eliminate the negative effects of the scanned scene.

The *SmartView Ring-light RL-100R60* and *RL-100IR50* (see Figure 5; Table 5), respectively, can be used for flash lightning and for permanent lightning as well. The light can be connected via programmable logic controller (PLC) output and turned ON/OFF according to the task requirements. It can be operated by Trigger signal as well, while the intensity can be controlled by pulse width modulation (PWM) signal if necessary.

Together with choosing light sources, it is necessary to select proper filters, which will be mounted on the front lens. The general reasons for optical filters application are to correct white balance; remove or allow infrared (IR), ultraviolet, or selected color range; remove undesirable reflections; get higher spatial resolution;²³ gamut; extend the scanning time, and so on.

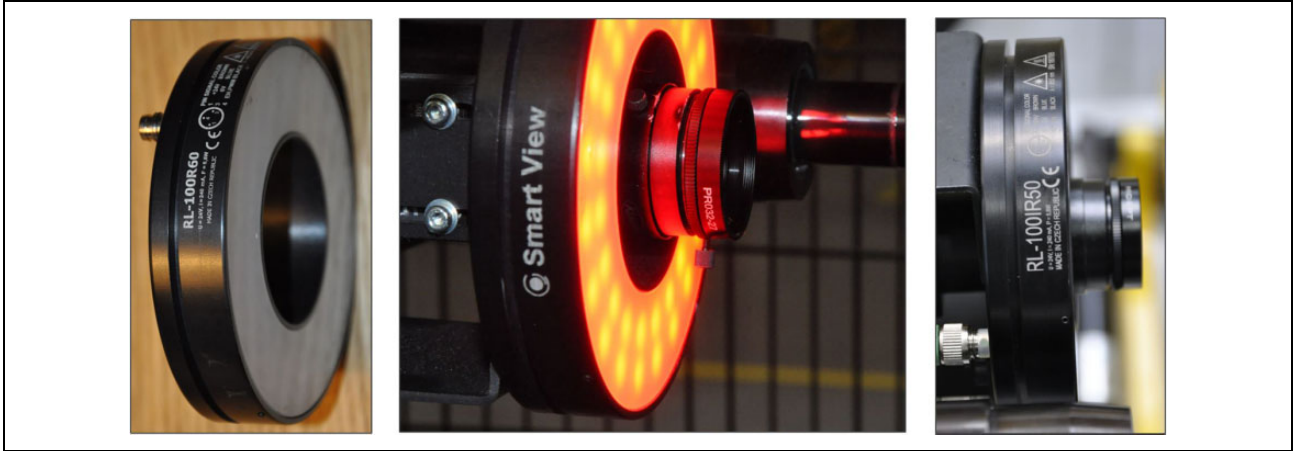


Figure 5. SmartView Ring-light RL-100R60 and RL-100IR50.

Table 5. Basic technical specification of *SmartView RL-100R60* and *RL-100IR50*.^a

Parameter	SmartView light type		
		RL-100R60	RL-100IR50
Voltage range	U_r	22–28 V	21–28 V
Nominal voltage/ nominal current	U_n/I_n	24 V DC/240 mA	24 V DC/240 mA
Maximum current	I_{\max}	240 mA	240 mA
Power	P	5.8 W	5.8 W
Trigger voltage/ trigger current	U_t/I_t	12–28 V/4.5 mA	12–28 V/3.5 mA
Light color/light wavelength	$-\lambda$	Red (R)/633 nm	IR/850 nm
Beam-width angle		60°	50°
Electric protection degree	IP	50	50
Safety class		III	III

IR: infrared.

^ahttps://www.smartview.cz/files/lights/data_sheet/smartview_datasheet_ring_cs.pdf.

MV filters were mounted on the front lens tube. Several individual filters and their combination have been tested (see Figures 5 and 6).

- Smart View RL-100R60 (red light) + filter Midopt BP635 (red light),
- Smart View RL-100R60 (red light) + filter/linear polarizer Midopt PR032-27,
- Smart View RL-100R60 (red light) + filter Midopt BP635 (red light) + filter/linear polarizer Midopt PR032-27,
- Smart View RL-100IR50 (IR) + filter Midopt BP635 (red light),
- Smart View RL-100IR50 (IR) + filter/linear polarizer Midopt PR032-27.

Best results were reached by IR ring light *Smart View RL-100IR50* combined with *light red bandpass filter BP635-27* and *linear polarizer PR032-27* (both are made by company Midwest Optical Systems, Inc.—MIDOPT, 322 Woodwork Lane Palatine, IL 60067 USA⁴²) mounted on the frontal lens.

Vision system setup

Next step is the tool *Vision Setup* via *iRVision WEB server* platform. In general, there exist two different approaches for measuring of objects position in VGR navigation—*absolute position measuring* and finding the data about *relative position offset* (*iRVision* adopts this approach). So, in our case, camera system provides the data about distance between object's *actual position* and the so-called *reference position*, and robot controller adjusts the final trajectory according to this distance.

On the one hand, the *iRVision* supports two kinds of robot position offset:³⁵

- *Fixed Frame Offset*—the object offset is measured in a coordinate frame fixed with respect to the robot base. An object placed on a fixed surface is viewed by a camera, and the vision system measures its position. The robot then adjusts its taught positions, so that it can find the object properly.
- *Tool Offset*—the workpiece offset is measured in a coordinate frame that moves with the robot tool. This method is useful for grippers where the part position in the gripper can vary, such as vacuum grippers. An object held by the robot is viewed by a camera, and the vision system measures its position relative to the gripper.

On the other hand, the following two types of camera mounting are selected:



Figure 6. Tested filtering elements—light red bandpass filter BP635-27 and linear polarizer PR032-27 and diffuser rings with different light transmission level.

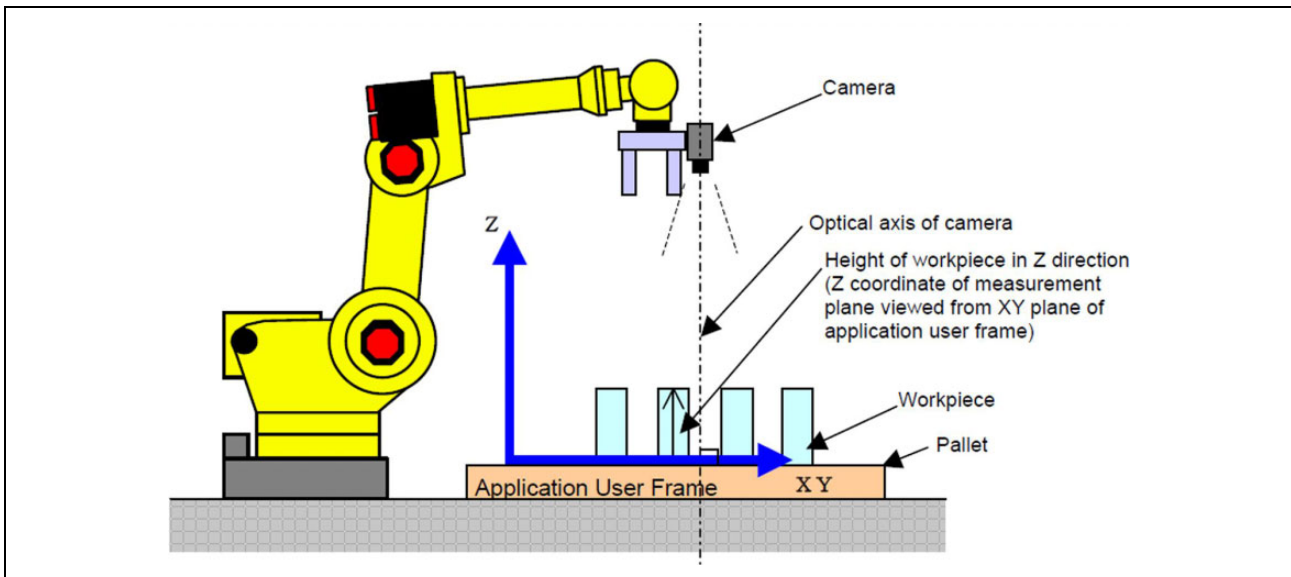


Figure 7. Principle of configuration “Robot-Mounted Camera + User Frame Offset.”³¹

- *Fixed Camera*—camera is connected to the static frame (e.g. over the scene),
- *Robot-Mounted Camera*—camera is carried on the robot arm.

Finally, there exist several possible combinations of both methods.

- Option 1: Fixed Camera + User Frame (UF) Offset (object is placed on the table),
- Option 2: Fixed Camera + Tool Frame Offset (object is placed in robot gripper),
- Option 3: Robot-Mounted Camera + UF Offset (camera is carried on the end effector and object is placed on the table).

With respect to the fact that the scanning process must be done from both left side and right side of the seat, we preferred option 3—Robot-Mounted Camera with UF offset. The principle of such configuration is shown in Figure 7.

The configuration procedure contains three steps (also the type of vision data), see Figure 8:

- *Camera Setup Tools*—camera configuration (port number, the type of the camera, the camera mounting method, etc.),
- *Camera Calibration Tools*—it establishes the mathematical correspondence between the camera coordination system and the world coordination system,
- *Vision Process Tools*—it defines the image processing, location, and measurement to be performed by iRVision during production operation.

“*Camera Setup Tool*”—*basic settings and camera configuration.* Control system recognizes the type and parameters of connected camera automatically. Furthermore, we can manually adjust the *focus ring* (according to expected working distance from the subject) and the *aperture control* (according to expected lighting conditions). You can also change the zoom setting with another lens type. However, this is not available or not necessary in our case. We will adjust

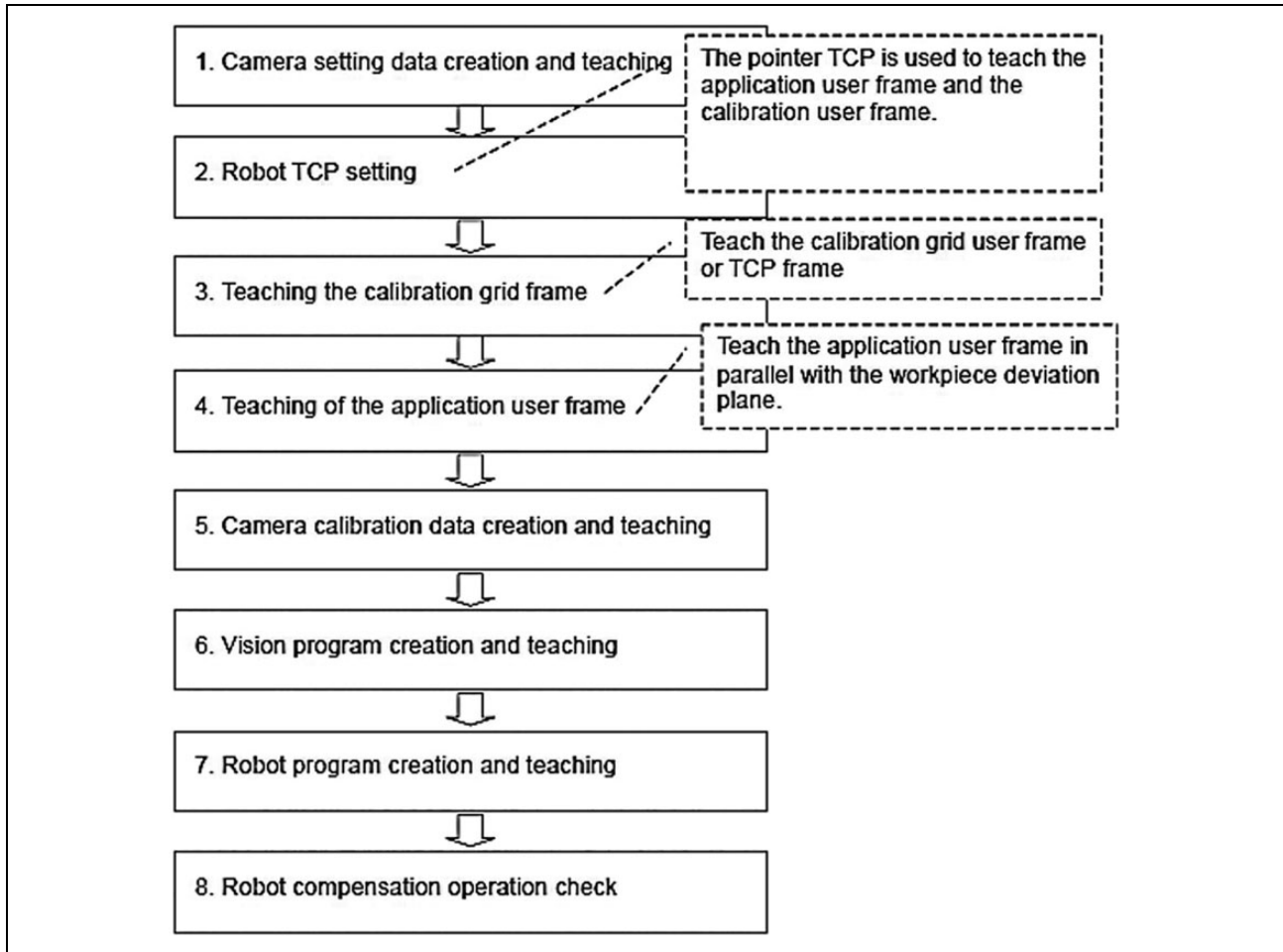


Figure 8. General schema of vision systems set-up procedure.³⁵

the working distance (chose the reference scanning position) to achieve a desired field of view (FOV) of approximately 150×150 mm for our application.

“Camera Calibration Tool”—basic settings. This step allows the robot control system to unify the relationship between the robot coordinate system and the camera FOV coordinate system. In case of FANUC robots, calibration is carried out by the means of the so-called 2D calibration grid with fixed spacing of optical calibration points (different sizes), in our case, 15×15 mm (Figures 9 and 10). Calibration is done with respect to a specific UF (in our case, UF2 or UF4, respectively; UF can be defined via three-point/four-point method). According to the used lens, the calibration projection can be defined—either orthogonal or perspective.

UFs definition. The UF defines the working space in which the robot works. The offset data from the vision system are all represented based on the UF. Therefore, it is very important to teach the UF as accurately as possible.

Table 6 lists all the defined UFs. We use UF6, 7, 8, and 9 for switching between LH and RH seat within the program.

The main difference between both seats lies in the horizontal shift 25 mm along the axis X (UF1). So, when the program for RH seat is running, the UF6 and 8 are loaded into UF2 and 4. While the program for LH seat is running, the UF7 and 9 are loaded into UF2 and 4. For such operation, the following instructions can be used:

1. PR [32] = UFRAME [7]; Loading the UF7 data into position register no. 32.
2. UFRAME [2] = PR [32]; Loading the position register no. 32 into UF2 (for LH).
3. PR [34] = UFRAME [9]; Loading the UF9 data into position register no. 34.
4. UFRAME [4] = PR [34]; Loading the position register no. 34 into UF4 (for LH).

In the case of a 2D vision application, the UF covers another important role. It defines the 2D work plane in the real 3D space. The 2D work plane for *iR*Vision must be parallel to the X–Y plane of the UF.

Each robot has different calibration requirements based on their applications, such as different cameras dependent on the type of vision system used which accompanies the

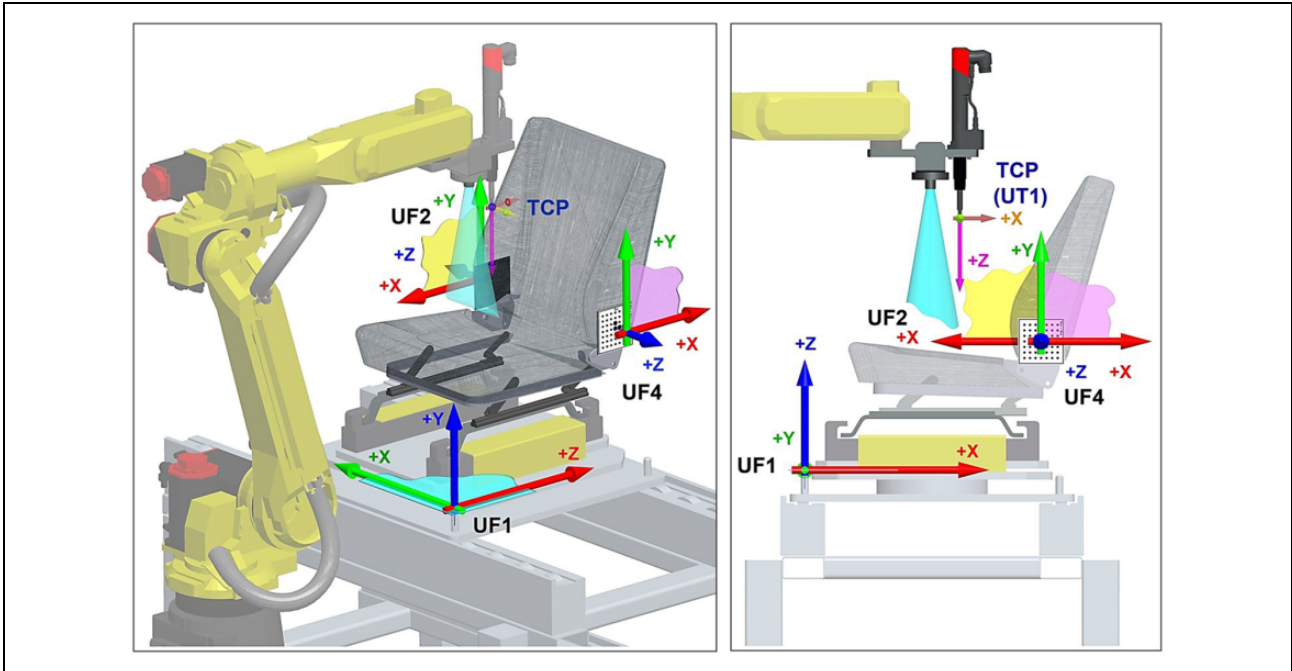


Figure 9. Defined UFs at the workcell. UF1: coordination system of the palette; UF2: coordination system of the left side (screws 1–4); UF4: coordination system of the right side (screws 2–3); UF: user frame.

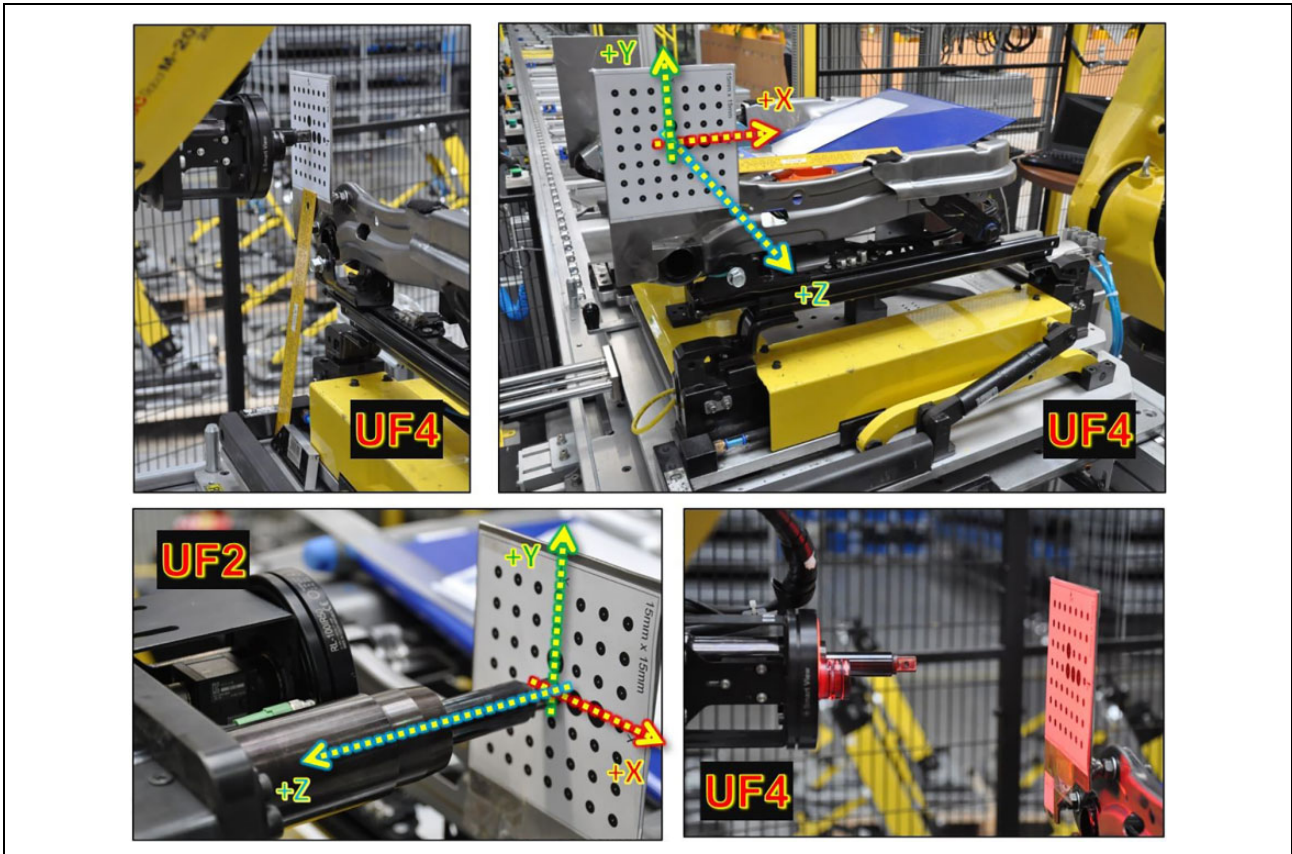


Figure 10. Calibration process—touching the calibration grid to define the origin of user frame 2/4.

Table 6. UF coordinates and configuration.

UF no.	UF coordinates and configuration (mm)					
UF1	X	635.656	Y	-352,058	Z	-25,631 SEAT_PALETTE
	W	0.215	P	-0,244	R	0,217 NUT 0 0 0
UF2	X	1248,291	Y	-264,158	Z	243,996 UF_Screw1-4
	W	89,928	P	-1,679	R	1,555 NUT 0 0 0
UF4	X	1233,702	Y	290,325	Z	243,652 UF_Screw2-3
	W	89,255	P	1,808	R	179,842 NUT 0 0 0
UF6	X	1248,207	Y	-289,158	Z	243,996 ORIGIN_UF2_RH
	W	89,928	P	-1,679	R	1,555 NUT 0 0 0
UF7	X	1260,992	Y	-212,202	Z	326,887 ORIGIN_UF2_LH
	W	89,470	P	-0,304	R	0,292 NUT 0 0 0
UF8	X	1238,526	Y	258,234	Z	243,545 ORIGIN_UF4_RH
	W	89,384	P	1,675	R	179,364 NUT 0 0 0
UF9	X	1258,648	Y	251,280	Z	323,496 ORIGIN_UF4_LH
	W	90,194	P	0,304	R	-179,468 NUT 0 0 0

UF: user frame.

Table 7. Calibration points for “two-plane method.”

Point	Point coordinates and configuration					
P2	Distance 325 mm between the end of the lens (without filters) and the grid					
	X	-90	Y	0	Z	250 Configuration
	W	180	P	0	R	180 NUT 0 0 0
P3	Distance 175 mm between the end of the lens (without filters) and the grid					
	X	-90	Y	0	Z	110 Configuration
	W	180	P	0	R	180 NUT 0 0 0

specific robot purchased.³⁶ Difficulties in the process of vision control developing process to cope with were:

- Localization of object of interest, in which the camera must be calibrated to locate the workpiece under the exposure area shown in Figure 4;
- Lighting conditions where the appropriate consistent lighting for the process must be determined prior to image collection;
- Image segmentation in which appropriate time segments must be utilized for the camera to collect quality images;
- Image quality as the black-and-white photography must be reviewed for high quality, and finally,

processing speed as higher processing speeds increases the efficiency of the process.⁷

Calibration for UF4 (screws 1 and 4, LH). We have done two separate *Camera Calibration Tools* for each seat from the “car set”:

- LH_Calbration_S_1and4_A,
- LH_Calbration_S_2and3_A,
- RH_Calbration_S_1and4_A,
- RH_Calbration_S_2and3_A.

The calibration method will then be described on the *LH_Calbration_S_1and4_A*. The same process was then repeated for all other calibrations. First of all, it is necessary to choose the fixture position—position of coordination system origin touched by the end effector (Figure 10). When we click the button “Set fixture position,” *iR*Vision system automatically calculates the grid position within UF (coordination system). Second step is choosing proper calibration position. The so-called two-plane method is recommended to prefer for Robot-Mounted Camera configuration (camera is carried on the robot end effector)—the calibration is done in two planes about 150 mm apart one another. This process can eliminate the optical distortion in optical elements and improve the precision of calibration data. The same process can be used when the camera is static and calibration grid is moving on the robot arm.

Calibration in first plane. We jog the robot into position P2 (Table 7), where the camera optical axis going through the UF4 origin in distance 325 mm measured from front edge of camera lens ring from calibration grid (Figure 11). Then we turned the light on and take the picture (SNAP button). When the grid is visible, the button FIND at “first plane” label can be used.

Calibration in second plane. We manually jog the robot into position P3 (Table 8, about 150 mm closer/farther from P2), then repeat the above steps for the second plane.

Calibration refinement—deleting points that flew out. The displayed distance between the centers of the green

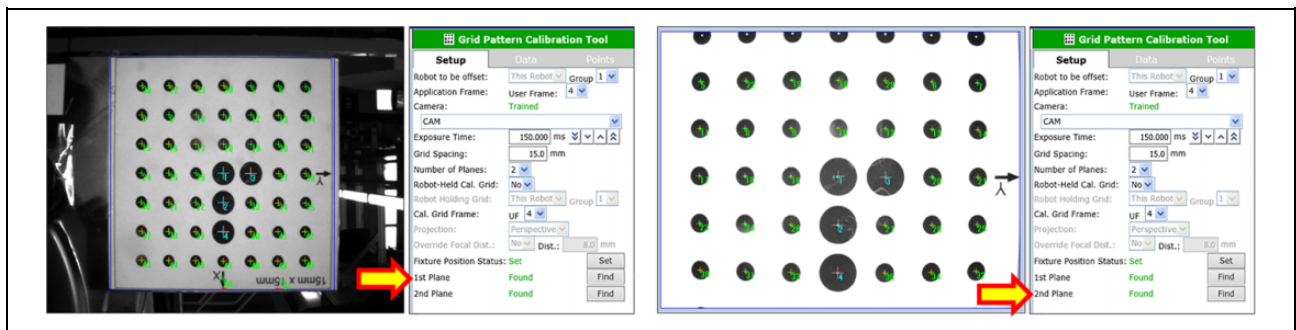


Figure 11. “Two-plane method” of calibration done by *iR*Vision system.

Table 8. Reference position P1 for screw no. 1, LH.

Reference position P1 for screw no. 1, LH						
PI	Reference position (3 mm between screwdriver tip and screwhead)					
X	-21.174	Y	-74.351	Z	0.001	Configuration
W	180	P	0	R	180	NUT 0 0 0

LH: code for left seat / left seat palette; NUT: code for robot specific configuration.

crosshairs and red crosshairs plotted on the image represents an error. A smaller value indicates more accurate calibration. If a crosshair is displayed at specific location where no grid point is present (Figure 12, left side), we can enter the index number of that point in the text box and then click the Delete button. The specified point is deleted from the list, and the calibration data are automatically recalculated (Figure 12, right side).

After this step, the calibration refinement for screws 1 and 4 can be considered as finished. The same process will be done for the second side of the seat—the grid for screws 2 and 3.

Vision process tools. The next step is to define *Vision Process Tool* for each search process separately—that means for each component, part, or feature. In our case, we have created a total of eight unique search tools with attribute as 2D-Single-View Vision Process Tool—each for one screw of LH seat/RH seat (see Figure 13):

- LH_SCREW_1_B_IRL/RH_SCREW_1_B_IRL— for the screw no. 1,
- LH_SCREW_2_B_IRL/RH_SCREW_2_B_IRL— for the screw no. 2,
- LH_SCREW_3_B_IRL/RH_SCREW_3_B_IRL— for the screw no. 3,
- LH_SCREW_4_B_IRL/RH_SCREW_4_B_IRL— for the screw no. 4.

At first, it is the definition of *GPM Locator Tool*—basically searching pattern definition. The next step is the parameters definition for pattern recognition according to the *GPM Locator Tool*. Setting the reference position, the offset value is calculated based on the relationship between the reference position and the current found position. In this step, the part height Z if the part position is above/below the application UF can be entered.

At the beginning, it was necessary to jog the robot to the required working position for each component. In our case, we navigate the robot to a position of 3 mm above the head of selected screw. Then, we remember the coordinates of given position into the control program as any standard point $P[n]$ (an example for P1 coordinates for screw 1, LH is listed in Table 8). This is how we got our reference location. Whenever a given object changes its position, the specific *Vision tool* is activated by *RUN_FIND* function, and the relative distance between the current and reference positions is measured and stored in the *Vision Register VR[n]* via *GET_OFFSET* function. Then, we apply the *VOFFSET VR[n]* function for specific point $P[n]$ in the program. If *RUN_FIND* function does not return a value

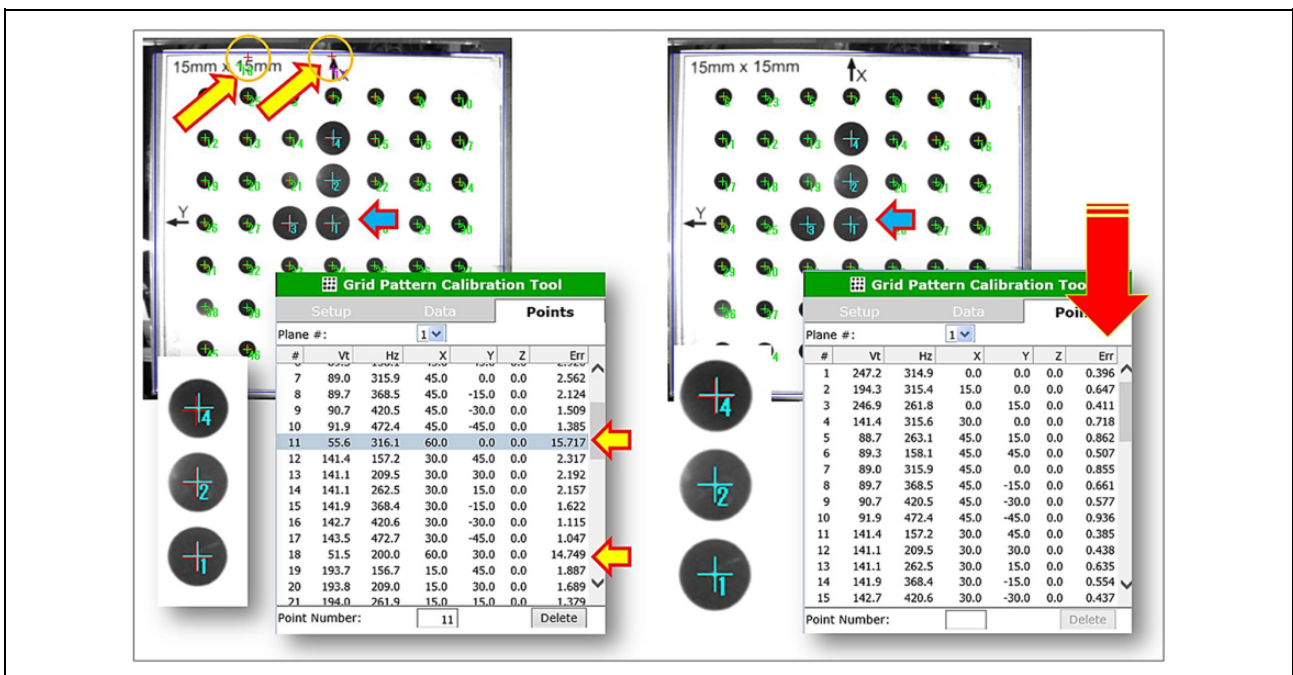


Figure 12. Calibration refinement—deleting points that flew out.

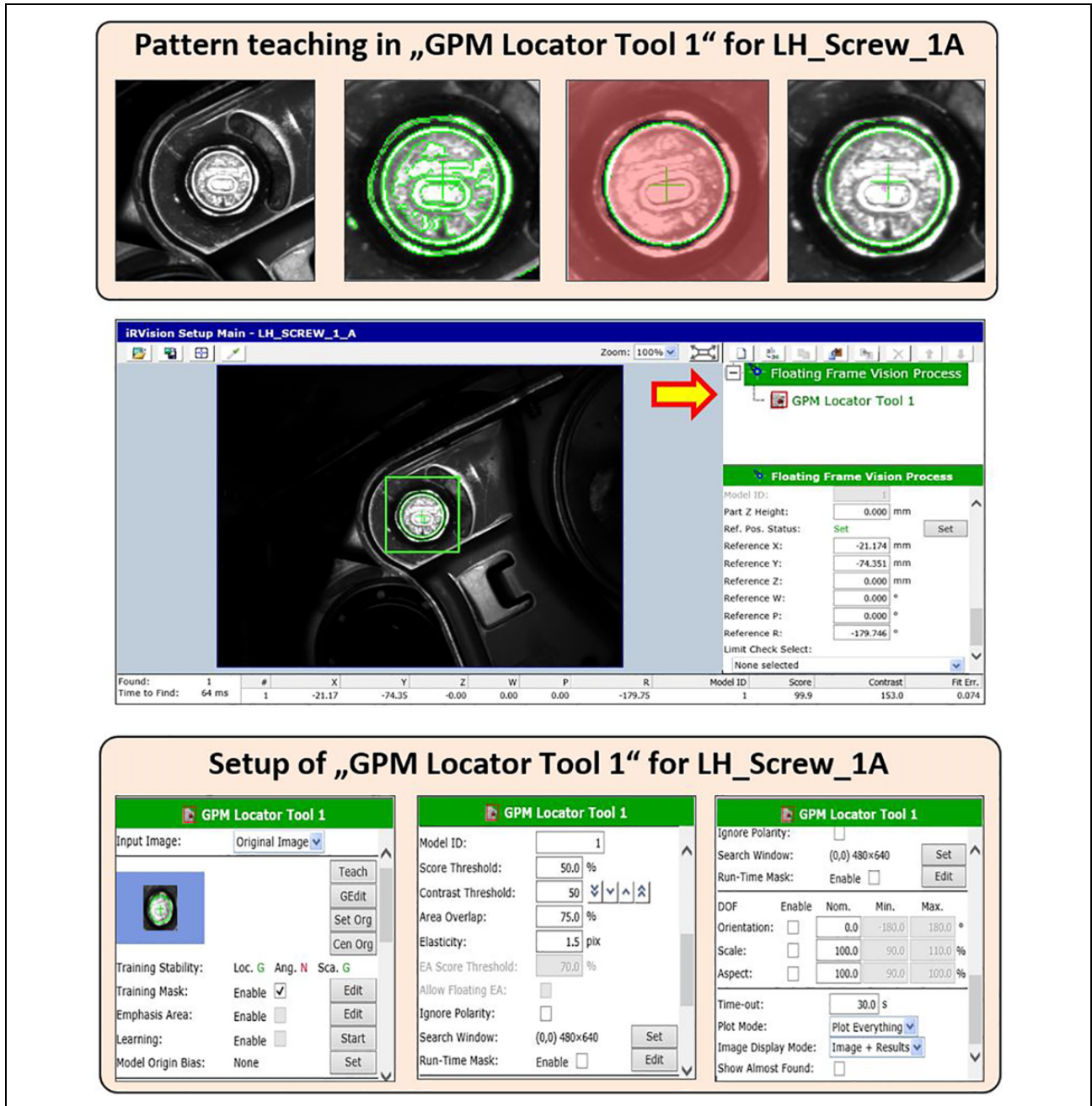


Figure 13. Setup process of 2D-Single-View Vision Process Tool for LR_SCREW_I_A: pattern teaching (up), pattern finding (middle), and setup of GPM Locator Tool parameters (bottom).

(the object is not found), the search process is repeated until the recognition is done successfully.

Experimental verification and improvement

During the experimental verification, we identified many factors which have different (positive or negative) influence for the recognition results as well as overall quality of screwing process. Further, we describe some experiment results.

Influence of the distance between camera lens and screwhead. At the beginning, the task definition contains requirement that all screws will come prescrewed from previous production sequence, but their exact position will depend on operator—so some seats will come with contact between screwhead and seat frame contact surface and some others will come with screws about 10 mm over the frame contact surface (only few revolutions). We have recognized that in some cases, there was negative influence of the distance between camera lens and screw + head (number of screw

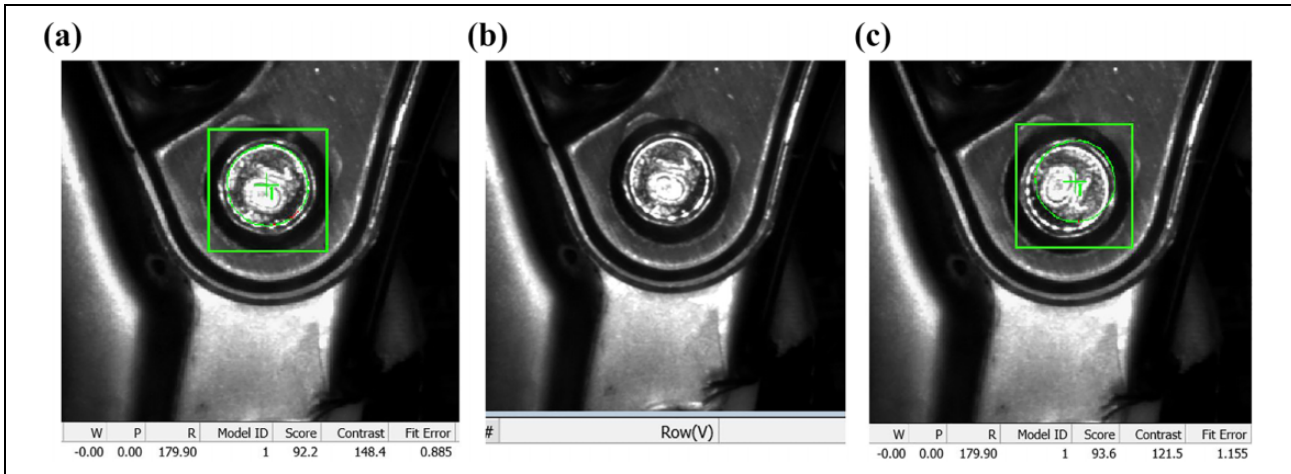


Figure 14. Influence of the distance between camera lens and screwhead: (a) Screwhead is about 5 mm over the metal frame. RH, screw 1: elasticity 1 pixel; distance between camera front lens and screwhead = 177 mm; (b) Screwhead is about 12 mm over the metal frame. RH, screw 1: elasticity 1 pixel; distance between camera front lens and screwhead = 170 mm; no detection; (c) Screwhead is about 12 mm over the metal frame. RH, screw 1: elasticity 4 pixel; distance between camera front lens and screwhead = 170 mm. RH: one right.

revolutions) on vision process (see Figure 14). It can be improved by elasticity (E) parameter. However, this solution is not completely sufficient.

This requirement was later changed—all seats are now entering the bolting station with contact between screwhead and seat frame contact surface and the robot unscrewing the screws about exactly defined number of revolutions and then screw them back until the requested torque was reached.

Influence of GPM Locator Tool parameters. In some cases, the detection system was not identifying objects correctly. So we decided to do several experiments; when we were changing these four parameters and examined their impact on the final behavior of designed GPM Locator Tool. Sometimes there was no pattern recognition or misinterpretation of image information when default settings were used.

Examples for different setting of GPM Locator Tool parameters are as follows:

- Score threshold (ST),
- Contrast threshold (CT),
- Area overlap (AO),
- Elasticity (E).

After several experiments, we can conclude that each parameter has, on the one hand, positive feedback, but at the same time, on the other hand, the negative influence on the recognizing results. Our experiences are shown in Figure 15.

We have seen that some amount of incorrect pattern identifications (searching of wrong objects) within camera focus area is caused by high number of circular objects in

camera range. There are two different ways how the searching area can be reduced only to desired location of the vision range (not whole picture will be analyzed).

- Run-Time Mask—specify an area of the search window that you do not want to be processed as an arbitrary geometry, such as a circle- or donut-shaped window;
- Search Window—specify the rectangular shape of the area to be searched. The default value is the entire image; it can be changed via Set Search Window button.

We defined the rectangular Search Window with the size of approximately 296×305 pixels. The preparing phase and experimental results are shown in Figure 16 and Table 9.

Range of horizontal and vertical seat adjustment. Other experiments prove very high influence of original screw position and range of its possible locations (Figures 17 and 18). This relation is caused by quite high light changings in the area of possible screw positions (see Figures 17 to 20).

The random unsuccessful recognition of screw 3 on RH seat during the testing phase was identified. We modified the program and vision system setup that in case of negative scan result (system repeating the scan up to 20 times and then send negative result), the control system shifts the robot arm about 10 mm to the side in X-axis (Table 10). This new position can help to reach better optical condition and find the screw position with higher accuracy (see Figure 21). This solution was evaluated after several months run as very successful and efficient.

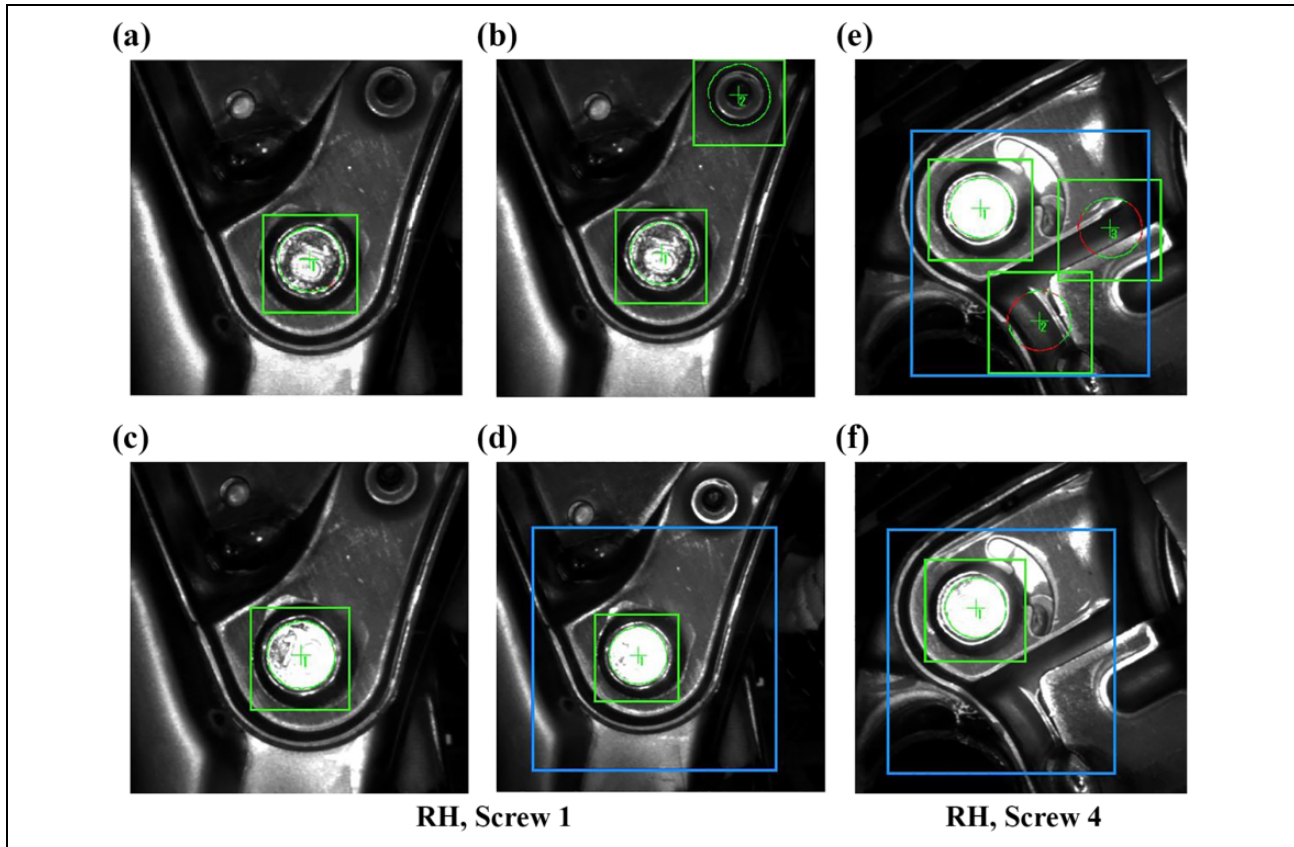


Figure 15. Influence of different setup of GPM Locator Tool parameters: (a) ST = 70%, CT = 50, AO = 30%, E = 2 pixel; (b) ST = 70%, CT = 50, AO = 30%, E = 5 pixel; (c) ST = 70%, CT = 50, AO = 30%, E = 2 pixel; (d) ST = 70%, CT = 50, AO = 30%, E = 2.5 pixel, Search Window; (e) ST = 40%, CT = 40, AO = 20%, E = 4 pixel; (f) ST = 80%, CT = 70, AO = 20%, E = 3 pixel, Search Window. ST: score threshold; CT: contrast threshold; AO: area overlap; E: elasticity.

Comparison of normal light and IR light source. As it was mentioned above about camera and lightning, two light sources, the red light and IR light, were tested (Figures 22 and 23). The results look not so far each other. A bit better results (more homogenous) were obtained by IR light source, for which we decided in final solution.

Conclusions and future work

Most of the large manufacturing companies, mainly from automotive industry, utilize integration of several systems into automated production lines. The different production facilities such as machine tools and industrial robots equipped with conveyors, pneumatic actuators, or vision systems can be considered as the core features of industrial automation. Utilizing more systems to work as one integrated system including quality control may be the solution to create quality product, increasing productivity and labor cost that result in company's long-term growth, and customer satisfaction.³⁶

Due to the ever-increasing variable nature of the production process caused by the increasing customization

level of the products, systems enabling the adaptability of production facilities are gaining importance.³⁵ Under these variable conditions, the vision identification of products, concretely the so-called MV systems or VGR systems, represents strong tools for robotics^{15,43} and starting to play a very significant role. However, in spite of their indisputable abilities, the resulting efficiency and successful application of the whole system depends on the quality of technical equipment, their mutual combination, and working condition, but above all on the quality of engineering work (knowledge and skills of the programmer).⁴⁴

We presented the case study about the development process and performance analysis of assembly system based on industrial robot FANUC M-20iA/20M with integrated iR-Vision system for screwing application in automotive industry in this article. The key feature of vision system is the designed robust and optimized recognition method obtained via detailed analysis of its setup and finding the best configuration of the whole system. The contribution of the presented system can be above all improved accuracy and efficiency. Unfortunately, due to the customer restriction, it is not possible to publish the real

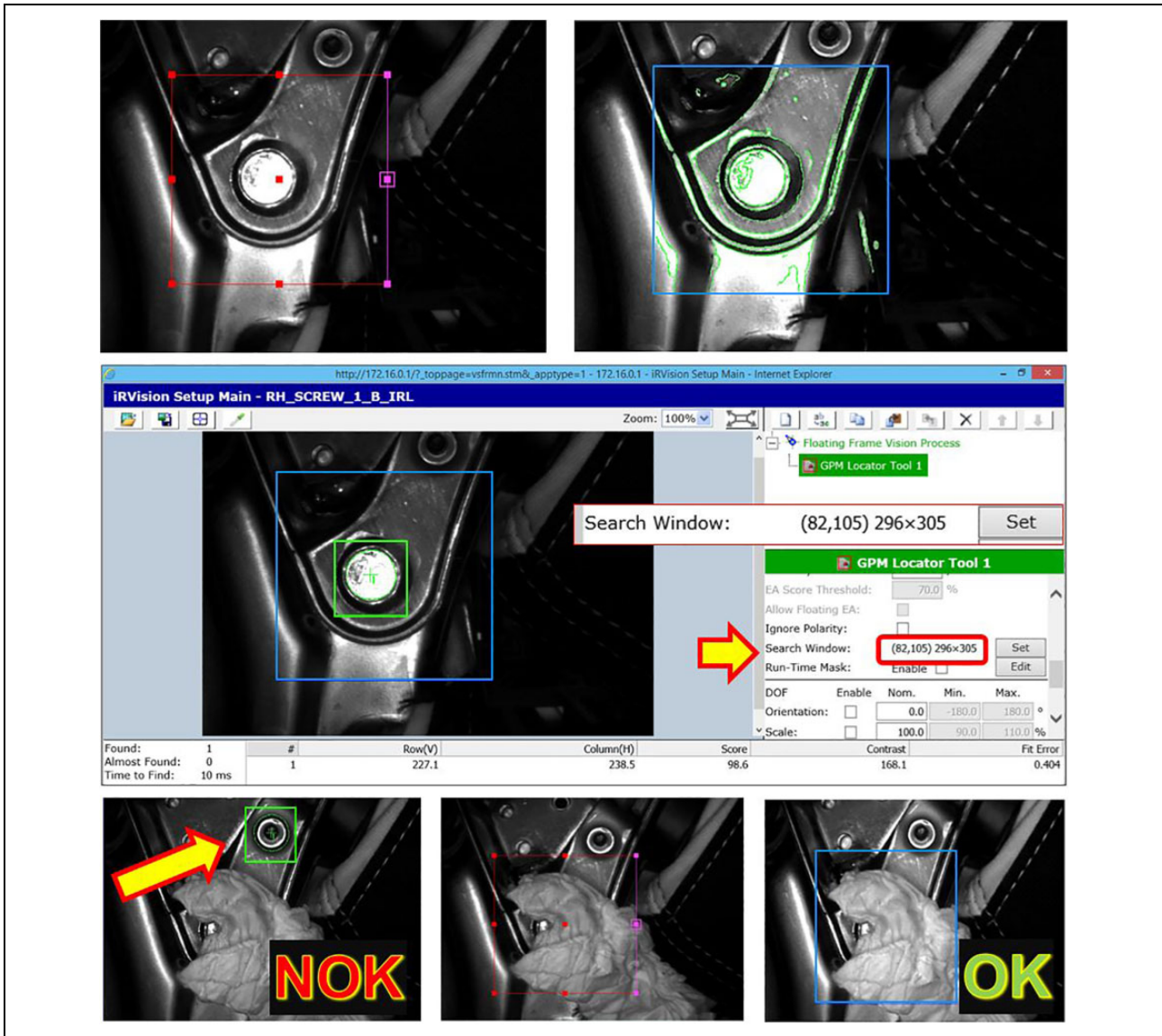


Figure 16. Reducing the searched area via Search Window tool and examples for NOK and OK results.

Table 9. Recommended and not sufficient value range of GPM Locator Tool parameters.

Parameter	Not sufficient value range		Recommended value range/best
	Bottom range	Upper range	
Score threshold	<70% (too weak/recognition of other objects as well)	>93% (too rigid/less percentage of successfully recognition)	70–93% (85%)
Contrast threshold	<40 (too weak/recognition of other objects as well)	>140% (too rigid/less percentage of successfully recognition)	50–140 (100)
Area overlap	<15 (too rigid/less percentage of successful recognition)	>30% (too weak/recognition of not fully circle shapes)—detection of screw behind an obstacle (!)	15–30% (20%)
Elasticity	1–2 pixels (too rigid/less percentage of successful recognition)	4–5 pixels (too weak/recognition of other objects as well)	2–4 pixels (2.5 pixels)
Search window	Defined < 100 × 100 pixels (too limited searching area)	Not defined = 480 × 640 pixels (recognition of other objects as well)	Defined size approximately 250 × 250 pixels

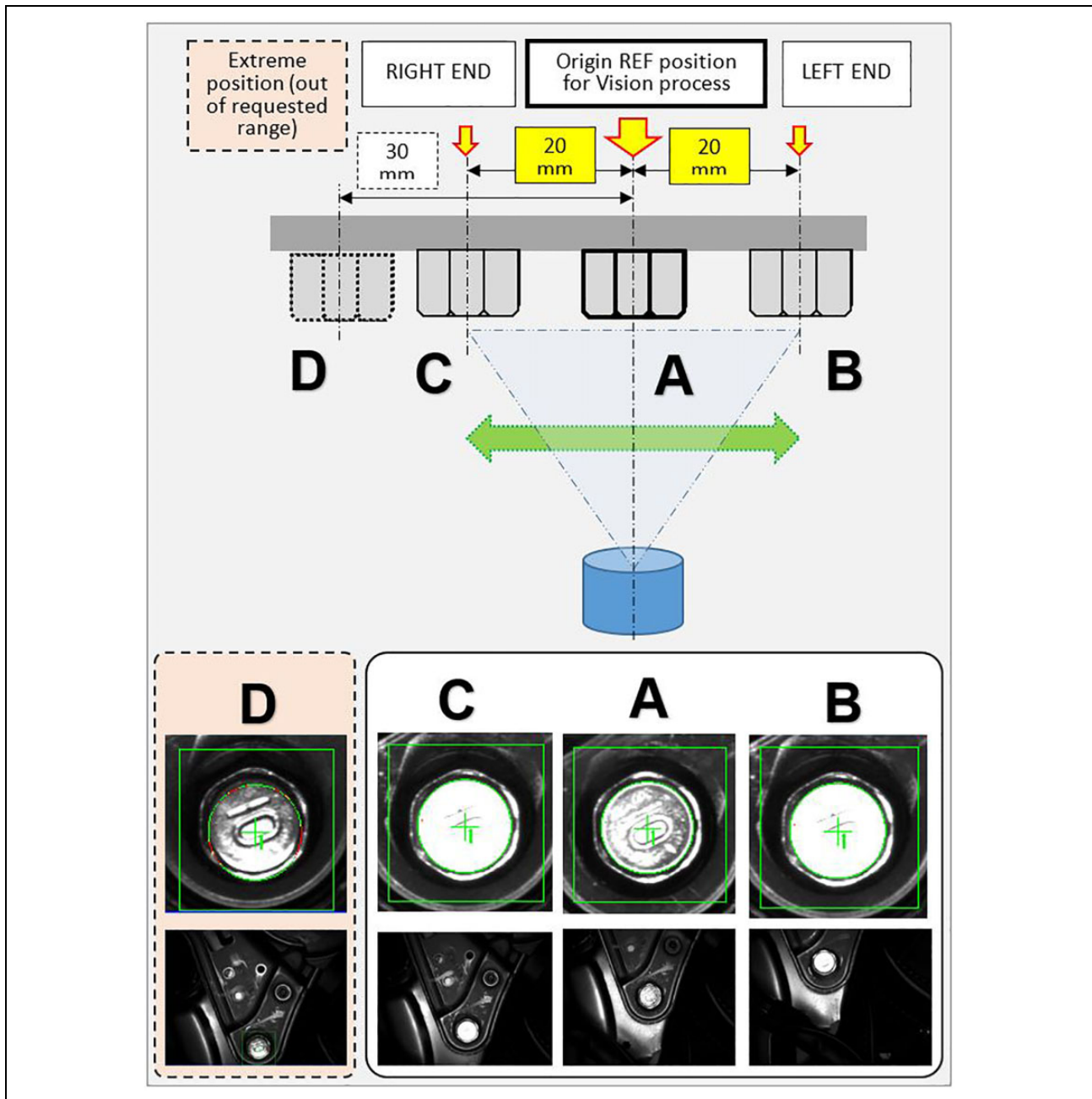


Figure 17. Changing quality of recognized pattern according to offset from reference (REF) position.

data from production statistics, to demonstrate the real influence of inaccuracies during the design process, to demonstrate the gradual “step-by-step” refinement, and to demonstrate the final influence of all changings on the final quality and efficiency of designed system. However, at the end of upgrade process, we reached the point where the total number of screwing operations with NOK results is less than required number, and it is about six single negative results per day (less than 0.1% NOK results; total process efficiency is higher than 99.9%). These NOK results are solved by next human operator.

The comparison before/after:

- *Before*—simple bolting work using system tool (1 worker/shift, total three workers);
- *After*—auto bolting using vision system; total 4 screws, location verification by vision reduce workers (1 worker/shift, total three workers);
- The skills of the engineering staff seem to be a crucial for final success, what was proved also in our experimental test.

The functionality of designed system was tested for approximately 2 years production run. During that period, the functionality of whole system and the

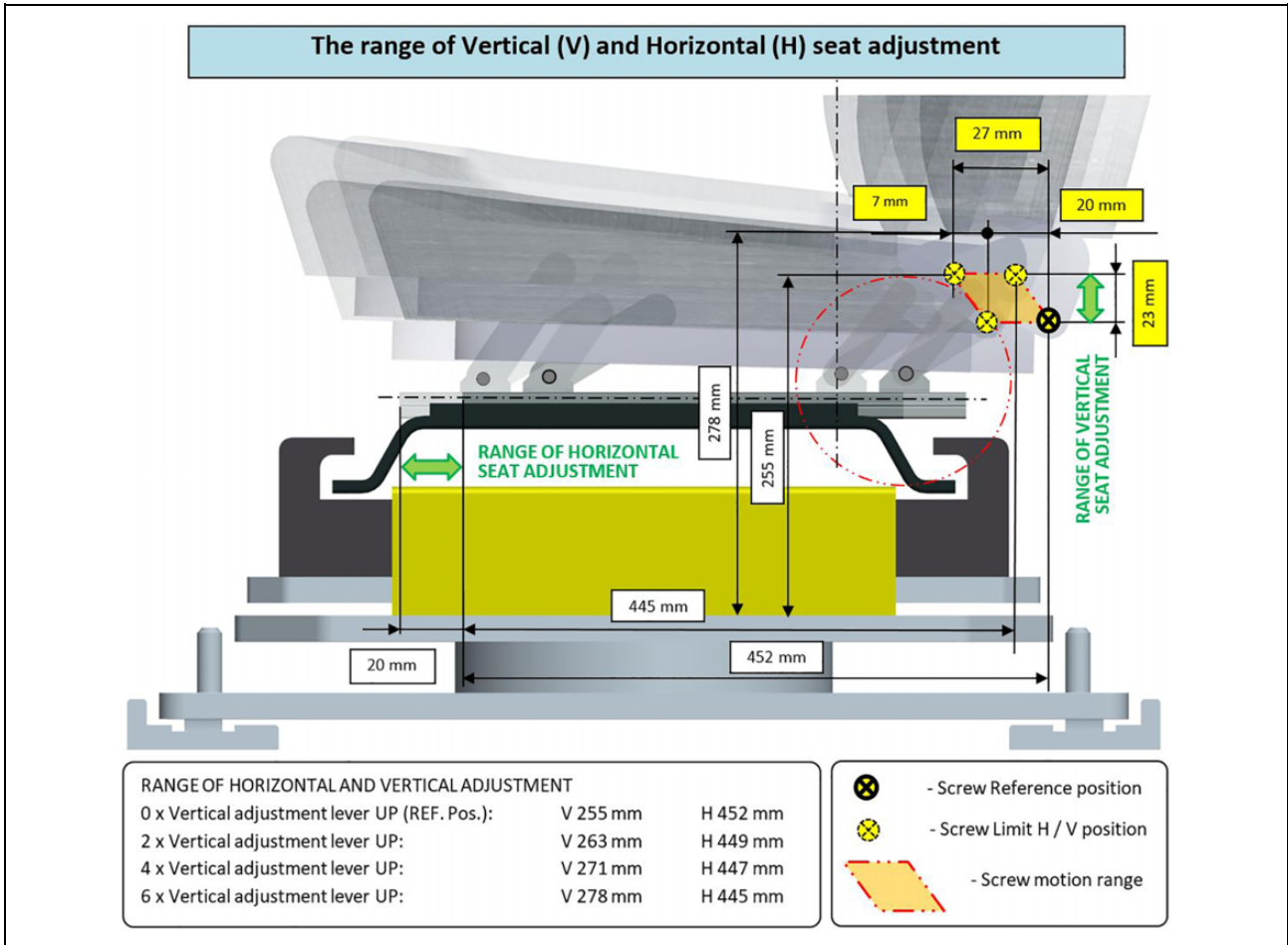


Figure 18. The range of vertical and horizontal seat adjustment.

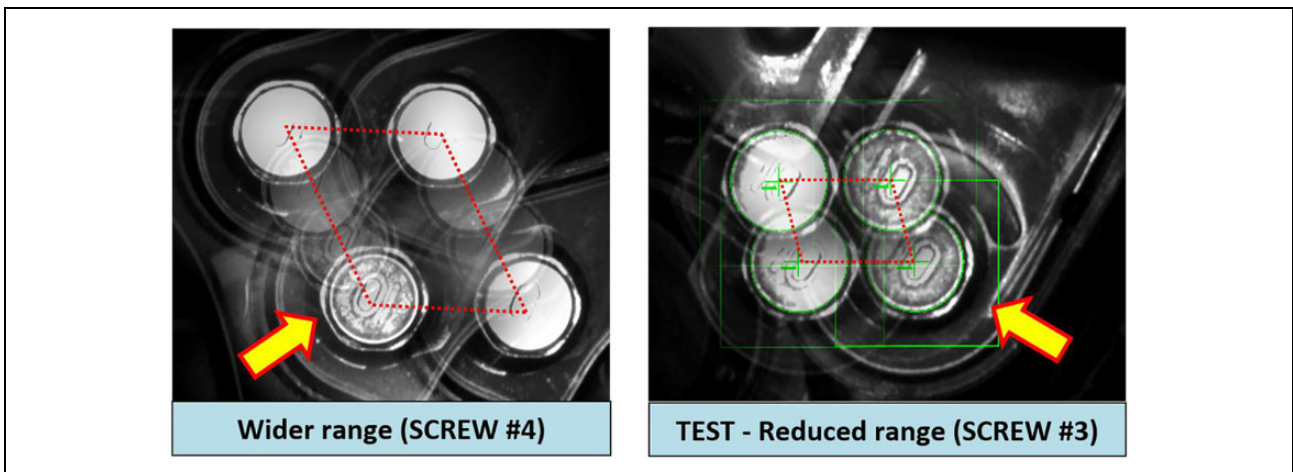


Figure 19. Influence of the seat adjustment range on pattern detection quality—camera snapshots, time-lapse during the seat adjustment motion.

functionality of each component were tested. First year was mainly focused on collecting as much as possible practical experiences and data about its behavior and mainly how the system can work under wide variety of conditions—light conditions, type of run, seat type

(manual/power, etc.), changing of human operators in working processes ordered before the bolting station, and so on. We have seen that some of our predictions were not met on both sides, as the main problem appears the changing of the light conditions. In general, it can be

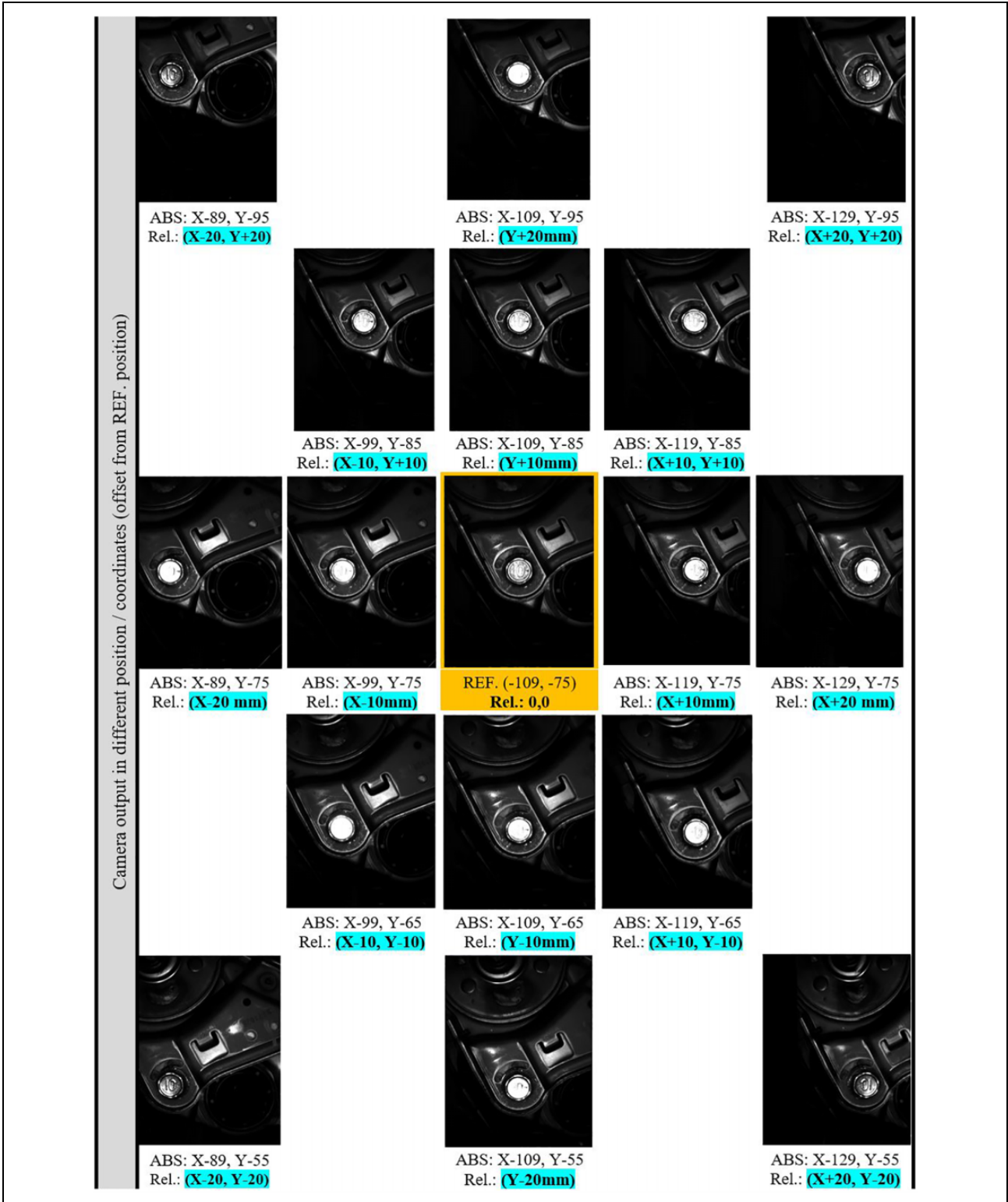


Figure 20. Camera output in different position/coordinates (offset from REF position).

considered as “the worst enemy” of sensitive VGR system. The light conditions were changed not only during the different part of the day, but even harder during the different season of the year due to the sun trajectory

with respect to the windows position in the factory main production hall (unfortunately, the customer doesn’t allow higher percentage of shadows or covering the bolting station). Another expectation that was not met

was on customer definition of the basic requirements, mainly cycle time parameter. It was analyzed that in case when the takt time of the production line was increased due to the previous undesirable interruption of the production (production line stopped regarding missing components, unplanned service work in some stations, or the robot needed to do repeating scanning several times per day), the robot wasn't able to increase

Table 10. Normal and shifted (bold; see X-coordinates) "rescan" position P5 for better pattern recognition.

Pos. no.	Position coordinates and configuration						
P5 (norm)	Distance 170 mm between the end of the lens (without filters) and the screw						
	X	-35	Y	-47	Z	93	Configuration
	W	180	P	0	R	-180	NUT 0 0 0
P5 (shift)	Distance 170 mm between the end of the lens (without filters) and the screw						
	X	-45	Y	-47	Z	93	Configuration
	W	180	P	0	R	-180	NUT 0 0 0

NUT: code for robot specific configuration.

its motion and bolting process itself and became a bottleneck of one assembly line segment. They finally redefine the original requirements on robot cycle time, changed from 35 s to less than 25 s (time START/STOP robot) or 45–34 s total cycle time of whole bolting station (time between two seats entering), respectively, what means the necessity to reach about 70% of projected cycle time. The application was tested in automatic regime when the recliner bolting station was able to reach the final cycle time of the robot at the level 21.3 s. So we can conclude that the problem with bottleneck was successfully solved. The experiments confirm our expectation as well as that the successful solution needed precise programming, setup, and exactly to know what is necessary to do.

Furthermore, on the experimental work basis, we can conclude that the successful application need precise analysis of each robotized workplace component, their behavior and interaction, and setup procedure, where all necessary parameters of VGR system are defined. The experimental work proves that:

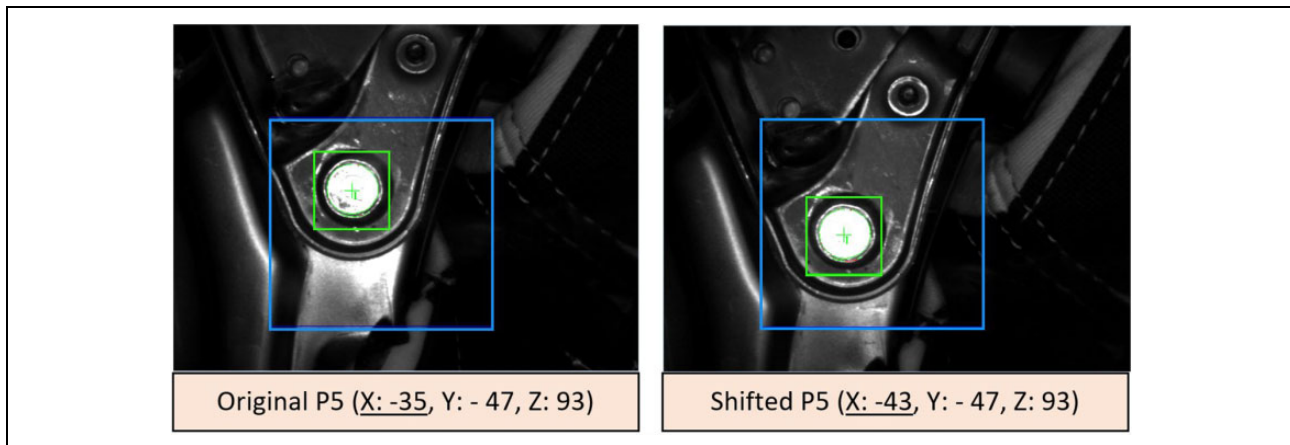


Figure 21. Original position P5 (X: -35), shifted position P5 (X: -43).

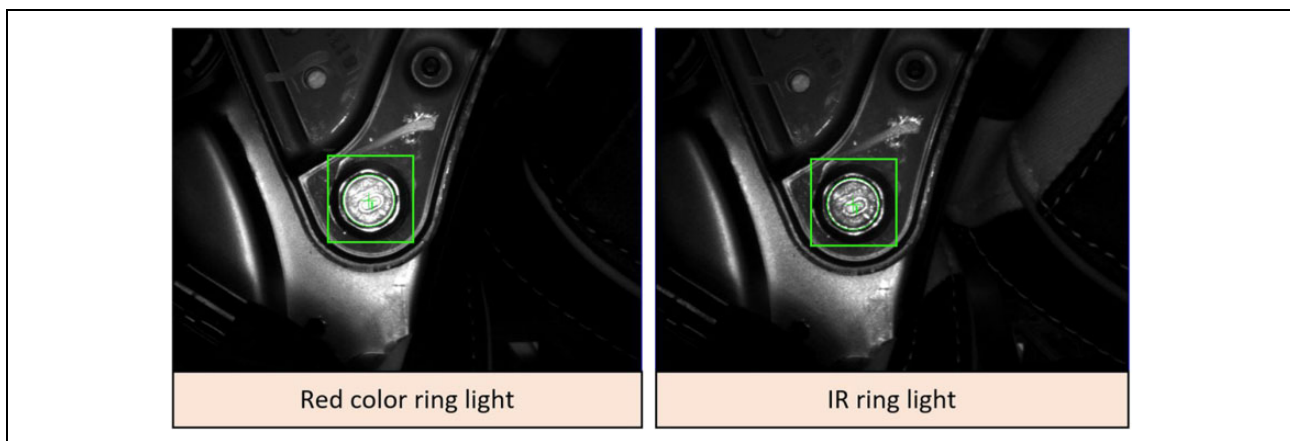


Figure 22. Results comparison between images obtained from standard red color ring light (left) and IR ring light. IR: infrared.

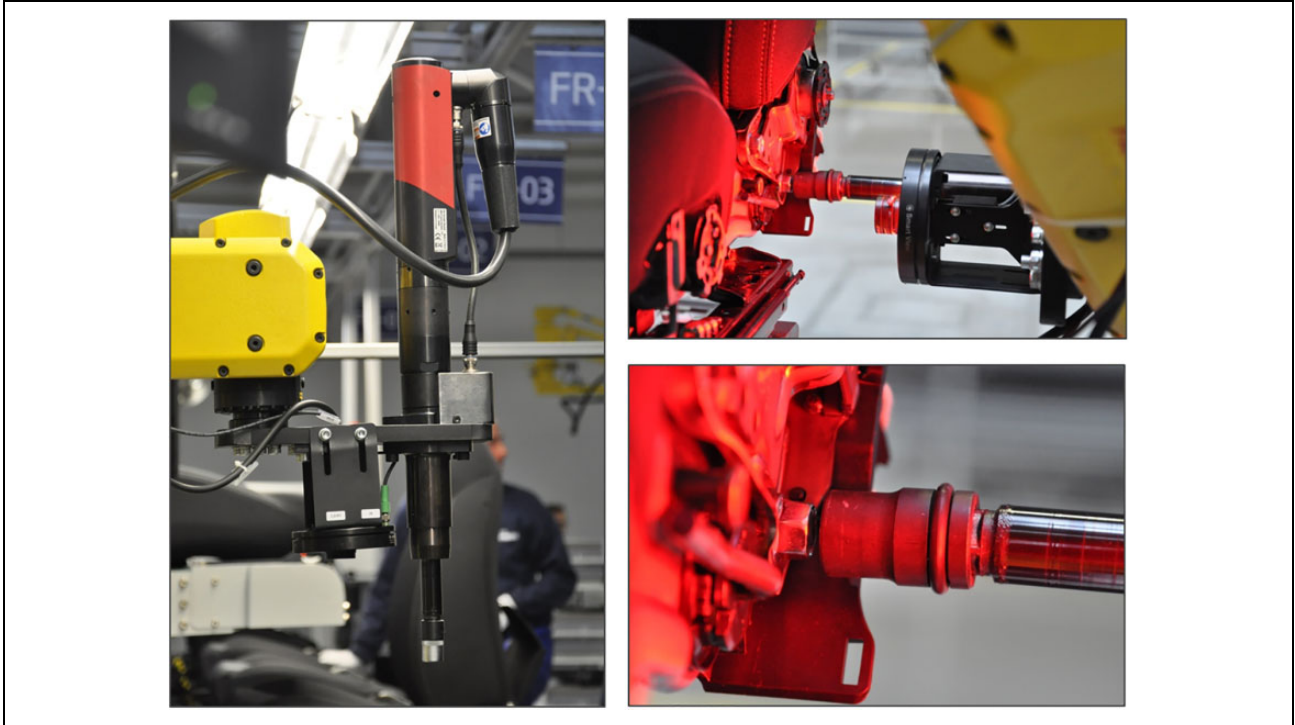


Figure 23. Experimental verification.

- in cases, the workcell can't be covered by any shadows and covering, the negative effect of the sun-light can be reduced via study of sun trajectory regarding the windows on walls/roof during whole year and at any part of the day;
- The IR light source (*SmartView RL-100IR50*), combined with proper filters (in our case *light red bandpass filter BP635-27* and *linear polarizer PR032-27*), can improve the detection about 10–20% (red light *RL-100R60* was tested as well);
- detailed analysis of object motion range within camera FOV and finding the optimal scanning position for pattern recognition seems to be the key element in such systems, which can dramatically reduce later development time and costs;
- for similar group of objects (screwheads), the better image results can be reached when optical axis of the camera is offset from screw axis. The screwhead reflections have significant influence positive/negative on detection quality;
- The setup procedure of VGR has significant influence on detection reliability, efficiency, and robustness. For similar applications, recommended values are $ST = 70\text{--}93\%$, $CT = 50\text{--}140$, $AO = 15\text{--}30\%$, $E = 2.5$ pixels, and reducing the searching area by Search Window function.

Finally, this article can help to other researchers to develop their own solutions for VGR assembly systems and avoid mistakes. We plan more detailed study of whole

recliner workcell and its continuous improvement for the future work.

Acknowledgements

The authors would like to thank companies AI engineers crowd, s.r.o., and Hyundai Transys Slovakia, s.r.o., both located in Slovak Republic for helping with practical implementation and experimental verification.



Declaration of conflicting interests

The author(s) declared no potential conflicts of interest with respect to the research, authorship, and/or publication of this article.

Funding

The authors disclosed receipt of the following financial support for the research, authorship, and publication of this article: This work is partially supported by the project APVV-16-0283: “Research and development of multi-criteria diagnosis of production machinery and equipment based on the implementation of artificial intelligence methods” and by grant agency VEGA, project No. 1/0073/19.

ORCID iDs

Vladimír Bulej  <https://orcid.org/0000-0001-8541-5827>
Ivan Virgala  <https://orcid.org/0000-0001-8273-2384>

References

1. Küpper D, Kuhlmann K, Köcher S, et al. The factory of the future. *BCG-Boston Consultin Group*. <https://www.bcg.com/publications/2016/leaning-manufacturing-operations-factory-of-future.aspx> (2016, accessed 10 October 2019).

2. Anadan TM. Advanced vision guided robotics. *Robotics Industry Insights*. https://www.robotics.org/content-detail.cfm/Industrial-Robotics-Industry-Insights/Advanced-Vision-Guided-Robotics-Technology-Trends-Impacting-VGR-Proliferation/content_id/3992 (2013, accessed 21 January 2019).
3. Dechow D. CD-automate 2011—the fundamentals of machine vision. *Automate 2011 Conference, McCormick Place*, Chicago, Illinois USA, 21–21 March 2011, CD-ROM Produced by World Class Tapes (TH_tutorial 19_Dave_Dechow_FINAL.pdf) (2011, accessed 2 November 2011).
4. Park JK, Kwon BK, Park J-H, et al. Machine learning-based imaging system for surface defect inspection. *Int J Prec Eng Manuf Green Tech* 2016; 3(3): 303–310.
5. Stejskal T, Kelemenova T, Dovica M, et al. Information contents of a signal at repeated positioning measurements of the coordinate measuring machine (CMM) by laser interferometer. *Measur Sc Rev* 2016; 16(5): 273–279.
6. Bayraktar E, Yigit C-B, and Boyraz P. A hybrid image dataset toward bridging the gap between real and simulation environments for robotics. *Mach Vis Appl* 2019; 30: 23–40.
7. Alghamdi B, Lee D, Scheffer P, et al. An integrated robotic system: 2D vision based inspection robot with automated PLC conveyor system. In: *Proceeding of the 4th international conference of control, dynamic systems, and robotics (CDSR'17)* (eds Ahmadi M and Nejat G) Toronto, Canada, 21–23 August 2017, Paper No. 136. pp. 1–10. Ottawa: ASET-AVESTIA Publishing. DOI: 10.11159/cdsr17.136.
8. Batchelor BG. Machine vision for industrial applications. In: Batchelor BG (ed) *Machine vision handbook*. Vol. 2. 1st ed. London: Springer-Verlag, 2012. pp. 1–59. DOI: 10.1007/978-1-84996-169-1_1.
9. Kim HH, Park JK, Oh J-H, et al. Multi-task convolutional neural network system for license plate recognition. *Int J Contr Autom Syst* 2017; 15(6): 2942–2949.
10. Park JK and Kang DJ. Unified convolutional neural network for direct facial keypoints detection. *Vis Comput* 2018; 35(11): 1615–1626. DOI: 10.1007/s00371-018-1561-3.
11. Kim JH, Yoon YZ, Yu S-C, et al. Real-time 2D height mapping method for an unmanned vehicle using a stereo camera and laser sensor fusion. *Int J Contr Aut Syst* 2012; 10(4): 761–771.
12. Ostertag O, Ostertagova E, Kelemen M, et al. Miniature mobile bristled in-pipe machine. *Int J Adv Rob Syst* 2014; 11(1): Art. No. 189.
13. Mikulova Z, Duchon F, Dekan M, et al. Localization of mobile robot using visual system. *Int J Adv Robot Syst* 2017; 14(5): 1–11.
14. Roberti F, Toibero JM, Soria C, et al. Hybrid collaborative stereo vision system for mobile robots formation. *Int J Adv Rob Syst* 2009; 6(4): 257–266. ISSN 1729-8806.
15. Lenhardt K. Optical systems in machine vision. In: Hornberg A (ed) *Handbook of machine and computer vision*. 2nd ed. Berlin: Wiley-VCH Verlag GmbH & Co. KGaA, 2017, pp. 179–290. DOI: 10.1002/9783527413409.ch4.
16. Kosinar M and Kuric I. Monitoring possibilities of CNC machine tools accuracy. In: *1st international conference on quality and innovation in engineering and management – QIEM 2011* (eds Popescu S, Brad S, and Popescu D), Cluj Napoca, Romania, 17–19 March 2011, pp. 115–118. Cluj-Napoca: Technical univ Cluj-Napoca. ISBN:978-973-662-614-2.
17. Stipancic T, Jerbic B, and Curkovic P. Context-aware system applied in industrial assembly environment. *Int J Adv Robot Syst* 2012; 9(234): 1–11. DOI: 10.5772/53235.
18. Scholz-Reiter B, Echelmeyer W, and Wellbrock E. Development of a robot-based system for automated unloading of variable packages out of transport units and containers. In: *2008 IEEE international conference on automation and logistics* (ed Xie), Qingdao, China, 1–3 September 2008, pp. 2766–2770. New York: IEEE. DOI: 10.1109/ICAL.2008.4636644.
19. Velisek K, Holubek R, Sobrino DRD, et al. Design of a robotized workstation making use of the integration of CAD models and Robotic Simulation software as way of pairing and comparing real and virtual environments. In: *4th international conference on computer and solution in management engineering 2016—COSME'16* (eds G. Oancea and MV Dragoi), Braşov, Romania, 3–4 November, 2016. Paper no: UNSP 05008. Book Series: MATEC Web of Conferences, Vol. 94, Les Ulis Cedex A: EDP Sciences. DOI: 10.1051/mateconf/20179405008.
20. He L, Dong Q, and Wang G. Fast depth extraction from a single image. *Int J Adv Robot Syst* 2016; 13: 11.
21. Liu Z, Wu S, Yin Y, et al. Calibration of binocular vision sensors based on unknown-sized elliptical stripe images. *Sensors* 2017; 17(2873): 1–17.
22. Miguel K, Brunete A, Hernando M, et al. Home camera-based fall detection system for the elderly. *Sensors* 2017; 17(2864): 1–21.
23. Bobovsky Z, Kryš V, and Mostyn V. Kinect v2 infrared images correction. *Int J Adv Robot Syst* 2018; 15 (1): 1–8.
24. Ghani MFA and Sahari KSM. Detecting negative obstacle using Kinect sensor. *Int J Adv Robot Syst* 2017; 14(3): 1–10.
25. Claer M, Ferrein A, and Schiffer S. Calibration of a rotating or revolving platform with a LiDAR sensor. *Appl Sci* 2019; 9(11): 2238.
26. Kocic J, Jovicic N, and Drndarevic V. Sensors and sensor fusion in autonomous vehicles. In: *26th Telecom Forum (TELFOR)* (ed Paunovic G), Belgrade, Serbia, 20–21 November 2018. Paper no. 136. pp. 420–425. New York: IEEE. DOI: 10.1109/TELFOR.2018.8612054.
27. Christie G, Kochersberger K, and Abbott AL. Fast inspection for size-based analysis in aggregate processing. *Mach Vis Appl* 2014; 26(1): 31–40.
28. Bozek P, Pokorny P, Svetlik J, et al. The calculations of Jordan curves trajectory of the robot movement. *Int J Adv Robot Syst* 2016; 13(5): 1–7.
29. Bako B and Bozek P. Trends in simulation and planning of manufacturing companies. *Procedia Eng* 2016; 149: 571–575.
30. Blatnický M, Dizo J, Blatnická M, et al. Design of a robot manipulator working screw revolutions. In: *23rd international conference on engineering mechanics 2017*, (ed Fuis V) Svratka, Czech Republic, 15–18 May, 2017, Book Series:

- Engineering Mechanics 2017, pp. 166–169. Brno: ACAD SCI Czech Republic.
31. Labudzki R, Legutko S, and Raos P. The essence and applications of machine vision. *Tech Gaz* 2014; 21(4): 903–909.
 32. FANUC—Industrial robots made for higher productivity. <http://www.fanuc.eu> (2018, accessed 27 July 2017).
 33. FANUC—Datasheet M-20iA-20M.pdf. <https://www.fanuc.eu/sk/en/robots/robot-filter-page/m-20-series/m-20ia-20m> (2017, accessed 27 July 2017).
 34. Desoutter. CVI3 range—EFDE-EFDA-EFDS fixtured electric spindles. <https://www.desouttertools.com/tools/2/electric-assembly-systems/21/cvi3-range/217/efde-efda-efds-fixtured-electric-spindles> (2017, accessed 5 October 2019).
 35. FANUC. FANUC robot series/R-30iA/R-30iB Mate CONTROLLER/iRVision—Operator’s Manual. B-82774EN/03. 14 September 2009. (iRVision_Operation_Manual_V7.50Pxx_[B-82774EN03].pdf). p. 460
 36. Dodok T, Cubonova N, and Kuric I. Workshop programming as a part of technological preparation of production. *Adv Sci Tech Res J* 2017; 11(1): 111–116. ISSN: 2299-8624.
 37. Ruzarovsky R, Holubek R, Sobrino DRD, et al. The simulation of conveyor control system using the virtual commissioning and virtual reality. *Adv Sci Tech-Res J* 2018; 12(4): 164–171.
 38. Bulej V, Stancek J, and Kuric I. Vision guided parallel robot and its application for automated assembly task. *Adv Sci Tech-Res J (ASTRJ)* 2018; 12(2): 150–157.
 39. FANUC—Vision functions for robots. <https://www.fanuc.eu/sk/en/robots/accessories/robot-vision> (2016, accessed 21 July 2017).
 40. Sony—progressive scan camera series. <https://www.image-sensing-solutions.eu/xc-56-brch.pdf> (2004, accessed 21 July 2017).
 41. Kang D-J, Ha J-E, and Jeong M-H. Detection of calibration patterns for camera calibration with irregular lighting and complicated backgrounds. *Int J Contr Aut Sys* 2008; 6(5): 746–754.
 42. Midopt—Choosing the best optical filter for your application. <https://www.stemmer-imaging.com/media/uploads/midopt/MI/MIDWEST-EN-Choosing-the-Best-Optical-Filter-for-your-Application.pdf> (2017, accessed 2 June 2019).
 43. Hrbcek J, Bozek P, Svetlik J, et al. Control system for the haptic paddle used in mobile robotics. *Int J Adv Robot Syst* 2017; 14 (5): 1–11.
 44. Xu Y, Gao F, and Jiang X. Performance analysis and evaluation of geometric parameters in stereo deflectometry. *Engineering* 2018; 4(6): 806–815.